Tanycyte-like cells derived from mouse embryonic stem culture show hypothalamic neural stem/progenitor cell functions

Mayuko Kano[a], Hidetaka Suga[a]*, Takeshi Ishihara[a,b], Mayu Sakakibara[a], Mika Soen[a], Tomiko Yamada[a], Hajime Ozaki[a], Kazuki Mitsumoto[a], Takatoshi Kasai[a], Mariko Sugiyama[a], Takeshi Onoue[a], Taku Tsunekawa[a], Hiroshi Takagi[a], Daisuke Hagiwara[a], Yoshihiro Ito[a], Shintaro Iwama[a], Motomitsu Goto[a], Ryoichi Banno[a] and Hiroshi Arima[a].

[a]Department of Endocrinology and Diabetes, Nagoya University Graduate School of Medicine, Nagoya, Aichi 466-8550, Japan

[b]Drug Discovery Technologies, Drug Discovery & Disease Research Laboratory, Shionogi and Co., Ltd., Toyonaka, Osaka 561-0825, Japan

Short title

Rax^+ tanycyte-like cells derived from mESCs

Key words

Mouse ES cells, tanycytes, retina and anterior neural fold homeobox, adult neural stem cells, hypothalamus

*To whom correspondence should be addressed.

Hidetaka Suga, M.D., Ph.D.

Department of Endocrinology and Diabetes

Nagoya University Graduate School of Medicine

65 Tsurumai-cho, Showa-ku, Nagoya 466-8550, Japan

Tel +81-52-744-2140, Fax +81-52-744-2212

E-mail: sugahide@med.nagoya-u.ac.jp

Financial Support

This work was supported by grants from the Project for Technological Development (H.S.) of the Research Center Network for Realization of Regenerative Medicine (RCNRRM), funded by the Japan Agency for Medical Research and Development (AMED); the Acceleration Program for Intractable Diseases Research utilizing Disease-specific iPS cells (H.S.) of RCNRRM funded by AMED; Grants-in-Aid for Scientific Research (H.S.) from The Ministry of Education, Culture, Sports, Science and Technology of Japan (MEXT); and Nagoya University Hospital Funding for Clinical Research (H.S.).

Disclosure Statement

The authors have nothing to disclose.

Abstract

Tanycytes have recently been accepted as neural stem/progenitor cells in the postnatal hypothalamus. Persistent retina and anterior neural fold homeobox (Rax) expression is characteristic of tanycytes in contrast to its transient expression of whole hypothalamic precursors. Here, we found that Rax^+ residual cells in the maturation phase of hypothalamic differentiation in mouse embryonic stem cell (mESC) cultures had similar characteristics to ventral tanycytes. They expressed typical neural stem/progenitor cell markers, including Sox2, vimentin, and nestin, and differentiated into mature neurons and glial cells. qRT-PCR analysis showed that Rax^+ residual cells expressed *Fgf-10*, *Fgf-18*, and *Lhx2* that are expressed by ventral tanycytes. They highly expressed tanycyte-specific genes *Dio2* and *Gpr50* compared with Rax^+ early hypothalamic progenitor cells. Therefore, Rax^+ residual cells in the maturation phase of hypothalamic differentiation were considered to be more differentiated and similar to late progenitor cells and tanycytes. They self-renewed and formed neurospheres when cultured with exogenous FGF-2. In addition, these Rax^+ neurospheres differentiated into three neuronal lineages (neurons, astrocytes, and oligodendrocytes) including neuropeptide Y $(NPY)^+$ neuron that are reported to be

differentiated from ventral tanycytes towards the arcuate nuclei. Thus, Rax^+ residual cells were multipotent neural stem/progenitor cells. Rax^+ neurospheres were stably passaged and retained high Sox2 expression even after multiple passages. These results suggest the successful induction of Rax^+ tanycyte-like cells from mESCs (induced tanycyte-like cells: iTan cells). These hypothalamic neural stem/progenitor cells may have potential in regenerative medicine and as research tool.

Introduction

Hypothalamic tanycytes are radial glial cell-like ependymal cells in the hypothalamus. Recent studies have reported that tanycytes are adult hypothalamic stem/progenitor cells (1-6) that play an important role in adult neurogenesis in the hypothalamus. Tanycytes also regulate feeding, weight, and energy balance via adult neurogenesis (1,7,8). Disruption of adult hypothalamic neural stem cells leads to impaired neuronal differentiation and ultimately the development of obesity and pre-diabetes (8). They gradually diminish with increasing age and are almost completely lost in old mice (4,5,9). Therefore, we considered that induction of tanycytes from pluripotent stem cells might be a new treatment approach for dysfunction of the hypothalamic homeostatic mechanism or energy regulation caused by disease and aging.

Tanycytes occupy the floor and lateral walls of the hypothalamic third ventricle (3V) and

73 extend long monopolar processes to the hypothalamic parenchyma (the arcuate and ventromedial
74 nuclei [ARC and VMH, respectively]) (6,10). They are traditionally classified into α1, α2, and β
75 tanycytes from the dorsal side of the tuberal hypothalamus (Fig. 1A). In addition to their
76 anatomical distributions, they are thought to have different morphological and physiological
77 properties and express different cell markers (1,3-6,10,11) (12) (Table 1). All tanycytes express
78 typical neural stem/progenitor cell markers including Sox2 and vimentin. Strong expression of
79 nestin has been observed in β tanycytes (1) (5).

80 The transcription factor retina and anterior neural fold homeobox (Rax), which functions
81 in hypothalamic and retinal development (13-15), is continuously expressed in tanycytes
82 (6,11,16,17). In the early stage of hypothalamic development, Rax is broadly expressed in
83 hypothalamic progenitors (16,18,19). By embryonic (E) day 16.5 in mice, Rax expression is
84 limited in the wall of the hypothalamic 3V and is absent from all other hypothalamic regions
85 (1,11,16). Tanycytes emerge during the same period that is the very end stage of hypothalamic
86 development (E17) (6,20,21). Therefore, tanycytes are thought to be the only area in the adult
87 hypothalamus expressing Rax.

88 Our colleagues established a three-dimensional culture method for embryonic stem cells
89 (ESCs) termed serum-free culture of embryoid body-like aggregates with quick re-aggregation
90 (SFEBq) (22). This method is appropriate for induction of various ectodermal derivatives from

ESCs. In this method, aggregates formed from ESCs exhibit self-organization and spontaneous formation of a highly ordered structure or patterning (23). Hypothalamic tissues have been generated from mouse ESCs (mESCs) and human pluripotent stem cells using the SFEBq method via Rax^+ hypothalamic progenitors (14) (24) (25) (26) (27). Another study efficiently induced Rax^+ hypothalamic progenitors from human induced pluripotent stem cells by combined early activation of sonic hedgehog signaling and NOTCH inhibition (28).

For mESCs, differentiation occurs efficiently when cultured in growth factor-free chemically defined medium (gfCDM). Strict removal of exogenous patterning factors during early differentiation is critical to induce rostral hypothalamic progenitors (14). The peak expression of Rax in this hypothalamic differentiation culture is approximately day 7. A large proportion of hypothalamic progenitor cells derived from mESCs express Rax (55%–70%) on day 7 (14). These Rax^+ cells show a progressive reduction in number along with hypothalamic neural maturation of arginine-vasopressin $(AVP)^+$ neurons at around days 20–25. However, we found that small Rax^+ areas remained even after the maturation of hypothalamic neurons. Therefore, we hypothesized that these Rax^+ cells in the maturation phase of hypothalamic differentiation are tanycyte-like cells in the postnatal hypothalamus.

Materials and Methods

Mouse ESC culture and hypothalamic neuronal differentiation

We used Rax-EGFP knock-in mESCs, an mESC line with EGFP cDNA knocked in at the Rax locus (14), established from a male mouse embryo. Undifferentiated mESCs were maintained on gelatin-coated dishes and passaged every 2–3 days (14) (22) (29). The maintenance medium of mESCs was Glasgow modified Eagle's medium (11710-035/Gibco) supplemented with 1% fetal bovine serum (FBS) (172012/Sigma, St. Louis, MO, USA), 10% KnockOut Serum Replacement (10828-028/Invitrogen, San Diego, CA, USA), 0.1 mM nonessential amino acids (11140-050/Gibco), 1 mM sodium pyruvate (25030-081/Gibco), 0.1 mM 2-mercaptoethanol (137-06862/Wako, Osaka, Japan), and 2000 U/ml LIF (ESG1107/Millipore, Bedford, MA, USA). Undifferentiated mESCs were maintained in medium containing 20 μg/ml blasticidin S (KK400/KNF, Tokyo, Japan) to eliminate differentiated cells. For hypothalamic induction, mESCs were dissociated into single cells by TrypLE Express (12605-010/Gibco) and quickly reaggregated in a 96-well low-cell-adhesion plate with U-bottomed wells (174929/Thermo, Waltham, MA, USA, 3,000 cells per 100 μl/well). From day 0 to 9, the medium was gfCDM consisting of 1:1 IMDM Glutamax (31980-030/Gibco)/F-12 Glutamax (31765-035/Gibco) containing 5 mg/ml purified BSA (A3156/Sigma), 1% Chemically Defined Lipid Concentrate (11905-031/Gibco), and 450 μM monothioglycerol (M6145/Sigma). On day 10, DFNB medium consisting of DMEM/F12 (D8900/Sigma) containing 3.85 g/l glucose (07-0680-5/Sigma), 1.2 g/l sodium hydrogen carbonate

(28-1850-5/Sigma), and 50 U/ml (for Penicillin) Penicillin/Streptomycin (15140-122/Gibco) supplemented with 1% N2 (17502-048/Gibco), 2% B27 (12587-010/Gibco), and 10 ng/ml CNTF (257-NT/R&D Systems, Minneapolis, MN, USA) was added to each well (100 µl/well). On day 13, the aggregates were transferred from the 96-well plate to a Millicell culture insert (MCSP06H48/Millipore) in DFNB with 10 ng/ml CNTF. Medium changes were performed every other day until cell sorting.

Cell sorting

Cells were sorted by a FACSAria cell sorter II (Becton-Dickinson, Franklin Lakes, NJ, USA). Data were analyzed by FACS Diva software (Becton-Dickinson). For cell sorting, aggregates on Millicell inserts were collected and dissociated into single cells using neuron dissociation solution S (297-78101/Wako). The cell suspension was filtrated through 5-mL Round-Bottom Tubes with a Cell Strainer Cap (38030/Falcon, NY, USA) before loading. Rax-EGFP^{+} and Rax-EGFP^{-} cells were gated by referring to scatter plots of the undifferentiated mESC population to avoid cross-contamination. The sorted cells were collected in sorting buffer (DMED/F12 with 1mM EDTA, and 1% FBS) containing 10 µM Y-27632 (034-24024/Wako) and 50 µg/ml DNase I (11284932001/Roche, Basel, Switzerland), and stored at 4°C until plating. For direct differentiation after sorting, sorted Rax-EGFP^{+} cells were resuspended in dissociation medium

containing DFNB, 10% FBS (SFBM30-2537/Equitech-Bio, Kerrville, TX, USA), 25 μg/μl BDNF (028-16451/Wako), 50 μg/μl NT-3 (141-06643/Wako), 0.5 μM LM22A-4 (SML0848/Sigma), and 10 μM Y-27632. Then, the cells were plated on PDL-coated glass coverslips (CG-14-PDL/neuVitro, Vancouver, WA, USA) in 24-well plates (142475/Thermo). On day 2, a medium change was performed with DFNB + 10 ng/ml CNTF and then every other day.

Neurosphere formation and maintenance

Sorted Rax-EGFP^{+} single cells were resuspended in DFNB medium supplemented with 20 ng/ml recombinant mouse FGF-2 (3139FB/R&D Systems), 20 ng/ml recombinant mouse EGF (2028-EG/R&D Systems), 10 μM Y-27632, and 2 μg/ml heparin (07980/Stem Cell Technologies, Vancouver, Canada). Then, they were seeded in ultra low binding 6-well plates (3471/Corning, NY, USA). Cell density was adjusted to 1.9×10^5 cells/3 ml DFNB medium/well. Cells were incubated at 37°C in a 5% CO_2 incubator. FGF-2 was added on day 2 or 3 (final concentration: 20 ng/ml). Cells self-formed many neurospheres by 2–3 days. Neurospheres were passaged every 5–7 days. For passage, the neurospheres were dissociated into single cells using neuron dissociation solution S and seeded as per the original conditions. To cryopreserve neurospheres, Cellbanker®1 (XR601/ZENOAQ, Fukushima, Japan) was used.

Neurosphere differentiation

For differentiation, the neurospheres were collected in a 15-ml centrifuge tube, centrifuged, and resuspended in dissociation medium. The medium containing neurospheres was seeded on PDL-coated glass coverslips in 24-well plates and incubated at 37°C in a 5% CO_2 incubator. On day 2, a medium change was performed with DFNB + 10 ng/ml CNTF and then every other day. On days 4–7, they were fixed for immunostaining.

SU5402 treatment and Rax-EGFP$^+$ neurosphere counting

The SU5402 treatment has been described previously (3). Sorted Rax-EGFP$^+$ cells were divided into three groups: DFNB + 20 ng/ml FGF-2, DFNB + 20 ng/ml FGF-2 and 20 μM SU5402 (572630/Millipore), and DFNB + 20 ng/ml FGF-2 and DMSO (D2650/Sigma, as the vehicle) and cultured in ultra low binding 24-well plates (3473/Corning). Images of Rax-EGFP$^+$ neurospheres were captured under a BZ-X700 microscope (Keyence, Itasca, IL, USA, RRID:SCR_016979) (30) on day 5 and merged using BZ-X Analyzer software (Keyence). The number of Rax-EGFP$^+$ neurosphere was counted by BZ-X700 Hybrid Cell Count Software (Keyence). In some cases, neurospheres were cultured in ultra low binding 24-well plates. Cell density was adjusted to 1×10^5 cells/1 ml DFNB medium/well. Images of neurospheres were captured under the BZ-X700 microscope on day 5 or 6 and merged using BZ-X Analyze software. The number of neurospheres

was counted using ImageJ software (NIH, Bethesda, Maryland, USA, RRID:SCR_003070) (31).

BrdU labeling

For BrdU labeling of neurospheres, 10 mM BrdU (B5002/Sigma) was added to neurosphere-medium on day 3 (final concentration: 10 μM). Cells were incubated at 37°C in a 5% CO_2 incubator for 48 h. Neurospheres were attached to PDL-coated glass coverslips in a 24-well plate. After 2–3 h, the medium was aspirated and the neurospheres were incubated in 1 N HCL (081-01091/Wako) for 1 h at room temperature (RT). They were washed three times in PBS and then fixed with 2% paraformaldehyde (PFA) for 10 min, followed by 4% PFA for 15 min before proceeding to immunohistochemistry.

Immunohistochemistry

Male mice were perfused with 4% PFA. Neurospheres were fixed with 4% PFA for 5–10 min. The cells on PDL-coated glass coverslips were fixed with 2% PFA for 10 min, followed by 4% PFA for 15 min. Dissected brain tissues were immersed in 30% sucrose (20% sucrose for cells) and embedded in O.C.T. Compound (4583/Sakura Finetek/Tokyo, Japan). They were cut into 10-μm-thick coronal sections using a cryostat. Immunohistochemistry was performed as described below. Sections (tissue or cells) were washed three times (15 min per wash) in 0.3% Triton-X 100/PBS

for permeabilization and then washed with PBS three times (15 min per wash). Subsequently, the sections were incubated in 2% (w/v) dry skimmed milk/PBS for 1 h at RT for blocking. Sections were incubated overnight at 4°C, with primary antibodies diluted in 2% dry skimmed milk/PBS. The next day, the sections were washed three times (15 min each wash) in 0.05% Tween 20/PBS and incubated with secondary antibodies diluted in 2% dry skimmed milk/PBS for 2 h at RT. Then, 4′,6-diamidino-2-phenylindole (DAPI; D523/Dojindo, Kumamoto, Japan) was added to visualize the cell nuclei. Subsequently, the sections were washed three times (15 min each wash) in 0.05% Tween 20/PBS and mounted in SlowFade™ Diamond (S36972/Thermo). For cells on PDL-coated glass coverslips, ProLong™ Diamond (P36970/Thermo) was used. Primary antibodies against the following molecules and dilutions were: AVP (T5048/Guinea pig/1:2000/Peninsula, San Carlos, CA, USA/RRID:AB_2313978) (32), BLBP (ab32423/Rabbit/1:100/Abcam, Cambridge, UK/RRID:AB_880078) (33), Bmi1 (ab14389/Mouse/1:200/Abcam/RRID:AB_2065390) (34), BrdU (sc-32323/Mouse/1:150/Santa Cruz, Dallas, Texas, USA/RRID:AB_626766) (35), CNPase (ab6319/Mouse/1:200/Abcam/RRID:AB_2082593) (36), pErk1/2 (4370/Rabbit/1:50/CST, Danvers, MA, USA/RRID:AB_2315112) (37), FGFR1 (9740/Rabbit/1:200/CST/RRID:AB_11178519) (38), GFP (04404-84/Rat/1:500/Nacalai, Kyoto, Japan/RRID:AB_10013361) (39), GFAP (AB5804/Rabbit/1:400/Millipore/RRID:AB_2109645) (40), GLAST (ab416/Rabbit/1:100/Abcam/RRID:AB_304334) (41), Ki67p (NCL-Ki67p/

Rabbit/1:500/Novocastra, Nussloch, Germany/RRID:AB_442102) (42), Lhx2 (GTX129241/Rabbit/1:200/Genetex, Irvine, CA, USA/RRID:AB_2783558) (43), MAP2 (AB5392/Chicken/1:10000/Abcam/RRID:AB_2138153) (44), MBP (MAB386/Rat/1:50/Millipore/RRID:AB_94975) (45), nestin (PRB315C/Rabbit/1:400/BioLegend, San Diego, CA, USA/RRID:AB_10094393) (46), NeuN (MAB377/Mouse/1:100/Millipore/RRID:AB_2298772) (47), Nkx2.1 (180221/Mouse/1:200/Zymed [Thermo]/RRID:AB_86728) (48), NPY (11976/Rabbit/1:3000/CST/RRID:AB_2716286) (49), O4 (MAB345/Mouse/1:200/Millipore/RRID:AB_11213138) (50), Olig2 (AB9610/Rabbit/1:500/Millipore/RRID:AB_570666) (51), Pax6 (PRB-278P/Rabbit/1:250/BioLegend/RRID:AB_291612) (52), POMC (H02930/Rabbit/1:400/Phoenix Pharmaceuticals, Burlingame, CA, USA/RRID:AB_2307442) (53), Rax (MS8407-3/Guinea pig/1:2000 [for tissue 1:500]/custom/ RRID:AB_2783560) (54), Rax (M229/Guinea pig/1:2000 [for tissue 1:500]/Takara, Shiga, Japan/RRID:AB_2783559) (55), SOX2 (GT15098/Goat/1:800 [for tissue 1:200]/Neuromics, Edina, MN, USA/RRID:AB_1623028) (56), Tuj1 (MMS435P/Mouse/1:10000/BioLegend/RRID:AB_2313773) (57), and vimentin (AB5733/Chicken/1:2000 [for tissue 1:1000]/Millipore/RRID: AB_11212377) (58).

Single cell intracellular immunostaining

For intracellular immunostaining of sorted single cells, Leucoperm™ (BUF09/Bio-Rad, Hercules, CA, USA) reagents were used. In brief, sorted cells were fixed with Reagent A and then permeabilized with Reagent B in the Leucoperm™ kit. Subsequently, the cells were incubated with primary antibodies for 30 min, washed with wash buffer (PBS containing 2.5% EDTA and 0.25% BSA), and then incubated with secondary antibodies for 30 min.

Evaluation of neural stem/progenitor cell markers in neurospheres.

To quantify $Sox2^+$ cells in neurospheres, we stained frozen sections of neurospheres and counted $Sox2^+$ cells at each passage. To evaluate the vimentin and nestin-positive rate, we dissociated 5th passage neurospheres into single cells. Subsequently, intracellular immunostaining was performed for cell counting.

Quantitative RT-PCR

Quantitative PCR (qPCR) was performed with five samples for the two groups using the Mx3000P Real-Time QPCR System (Agilent Technologies, Santa Clara, CA, USA). The data were normalized to *Gapdh* mRNA expression. Primers used were as follows: *Gapdh*, forward 5′-TGACCACAGTCCATGCCATC-3′, reverse 5′-GACGGACACATTGGGGGTAG-3′; *Rax*,

253 forward 5′-GTTCGGGTCCAGGRATGGTT-3′, reverse 5′-GAGAGGAGGGGAGAATCCTG-3′;
254 *Lhx2*, forward 5′-CCTACTACAACGGGCGTGGGCACTGT-3′, reverse 5′-
255 GTCACGATCCAGGTGTTCAGCATCG-3′; *Fgf-10*, forward 5′-
256 GCCACCAACTGCTCTTCTTC-3′, reverse 5′-CTCTCCTGGGAGCTCCTTTT-3′; *Fgf-18*,
257 forward 5′-CTTGCACTTGCCTGTGTTTA-3′, reverse 5′-AGCCCACATACCAACCAGAC-3′;
258 *Vim*, forward 5′-GGGGGATGAGGAATAGAGGCT-3′, reverse 5′-
259 GGGGGATGAGGAATAGAGGCT-3′; and *Nes*, forward 5′-GAGAAAGAGAATCAGGAGCC-3′,
260 reverse 5′-CAAGAGACCTCAGAGATTCC-3′; *Dio2*, forward 5′-
261 GCTTCCTCCTAGATGCCTACAA-3′, reverse 5′-CCGAGGCATAATTGTTACCTG-3′; *Gpr50*,
262 forward 5′-AGAGCAACATGGGACCTACAA-3′, reverse 5′-
263 GCCAGAATTTCGGAGCTTCTTG-3′; *Ppp1r1b*, forward 5′-AGATTCAGTTCTCTGTGCCCG-
264 3′, reverse 5′-GGTTCTCTGATGTGGAGAGGC-3′; *Cldn1*, forward 5′-
265 CTGGAAGATGATGAGGTGCAGAAGA-3′, reverse 5′-CCACTAATGTCGCCAGACCTGAA-
266 3′.
267
268 **Imaging**
269 Immunohistological imaging was carried out using an FV1200 Laser Scanning Microscopes
270 (Olympus, Tokyo, Japan, RRID:SCR_016264) (59). Images of Rax-EGFP^{+} neurospheres were

captured using an AXIO Zoom V16 Fluorescence Stereo Zoom Microscope (Zeiss, Oberkochen, Germany, RRID:SCR_016980) (60). Images were processed with Adobe Photoshop (Adobe Systems Incorporated, San Jose, CA, USA, RRID:SCR_014199) (61).

Statistical analyses

IBM SPSS Statistics (IBM, Armonk, NY, USA, RRID:SCR_002865) (62) was used for statistical analyses. The two-tailed unpaired *t*-test was used for two-group comparisons of Rax-EGFP^{+} and Rax-EGFP^{-} mRNA expression, and Rax-EGFP^{+} and early hypothalamic progenitor mRNA expression. The two-tailed unpaired Student's *t*-test was used for analyses of *Fgf-10*, *Lhx2*, *Vim*, *Nes*, *Gpr50* (Rax-EGFP^{+} and early hypothalamic progenitor), *Ppp1r1b,* and *Cldn1* mRNAs. The two-tailed unpaired Welch's *t*-test was used for analyses of *Rax*, *Fgf-18*, *Gpr50* (Rax-EGFP^{+} and Rax-EGFP^{-}), and *Dio2* mRNAs. The numbers of neurospheres in the two groups [FGF-2(+) and FGF-2(-)] were analyzed by Student's *t*-test. The numbers of neurospheres in the three groups (FGF-2, FGF-2+Vehicle, and FGF-2+SU5402) were analyzed by one-way ANOVA followed by Tukey's test. Rax^{+} cells in 6th passage neurospheres treated with or without FGF-2 were analyzed by the Mann–Whitney *U*-test. $P < 0.05$ was considered as statistically significant (*$P < 0.05$ and **$P < 0.01$).

289 **Results**

290 ***In vitro* Rax-EGFP$^+$ cells express neural stem/progenitor cell markers and differentiate into**

291 **neurons and astrocytes**

292 Rax expression was observed along with the 3V walls as reported previously (Fig. 1B)

293 (1,11,16). Typical neural stem/progenitor cell markers, such as Sox2 and vimentin, were expressed

294 in all tanycytes (Fig. 1C, D), whereas nestin was expressed mainly in β tanycytes (Fig. 1E).

295 We used a Rax-EGFP knock-in mESC line (EB5, clone 20-10) that allowed EGFP to be

296 used as a marker for Rax-expressing cells (14). Using the SFEBq method (Fig. 1F), mESCs

297 spontaneously differentiated into hypothalamic nerves and glial cells via Rax$^+$ hypothalamic

298 progenitor cells (Fig. 1G). In the late-phase of hypothalamic differentiation, there were numerous

299 hypothalamic neurons positive for AVP, neuropeptide Y (NPY), and pro-opiomelanocortin

300 (POMC) (Fig. 1H–J). Rax-EGFP expression reached a peak at day 7 (Fig. 1G) and then

301 subsequently diminished. However, small Rax-EGFP$^+$ areas were sustained within the aggregates

302 even after hypothalamic neurons and glial cells completed their differentiation (Fig. 1K). In

303 addition, some Rax-EGFP$^+$ cells had process-like structures, although they were both unipolar and

304 bipolar (Fig. 1L, M).

305 We isolated Rax-EGFP$^+$ cells by cell sorting from day 22 to 25 (Fig. 1F) when

306 hypothalamic neurons and glial cells had already differentiated. The proportion of Rax-EGFP$^+$

cells was reduced to 14.8 ± 0.94% (mean ± s.e.m., n=36) on days 22–25 compared with day 7. Therefore, the Rax-EGFP$^+$ area was more limited in the late stage of hypothalamic differentiation compared with the early stage. The sorted Rax-EGFP$^+$ cells expressed Sox2, vimentin, and nestin that are representative neural stem/progenitor cell markers (Fig. 2A–G). The Rax-EGFP$^+$ cells also expressed Lhx2 (Fig. 2H) that was previously reported to play a central role in the terminal differentiation of tanycytes by maintaining Rax expression in tanycyte progenitors (63).

When Rax-EGFP$^+$ cells were attached to PDL-coated glass coverslips, they differentiated into MAP2$^+$ NeuN$^+$ mature neurons (64) or GFAP$^+$ astrocytes (65) (Fig. 2I, J). Some neurons expressed the orexigenic neurotransmitter, NPY, which differentiated from ventral tanycytes towards ARC (1,4) (Fig. 2K). There were no oligodendrocytes differentiated from Rax-EGFP$^+$ cells.

These results indicated that the Rax-EGFP$^+$ cells remaining in the late phase of hypothalamic differentiation were neural stem/progenitor cells that could differentiate into both neural and glial cells, although their differentiation ability was limited to two neuronal lineages.

Rax-EGFP$^+$ cells express ventral tanycyte markers including FGF

Next, we examined mRNA expression in Rax-EGFP$^+$ cells (Fig. 3A–L). The mRNA levels of several ventral tanycyte markers, such as fibroblast growth factor (*Fgf*)-*10*, *Fgf-18*, and

325 *Lhx2*, were significantly increased in Rax-EGFP$^+$ cells (Fig. 3B–D). *Fgf*-10 was detected in ventral
326 α2 tanycytes (vα2 tanycytes) and β tanycytes (3,4,66), and *Fgf*-18 was present in vα2 tanycytes
327 (3) (Table 1). Strong *Lhx2* expression has also been reported in β tanycytes (1,63). In addition, the
328 expression levels of tanycyte-specific genes, such as iodothyronine deiodinase type 2 (*Dio2*) (67)
329 (68) (69) and G protein-coupled receptor 50 (*Gpr50*) (11,70) (12), were significantly increased in
330 Rax-EGFP$^+$ cells (Fig. 3E, F). Vimentin (*Vim*) and Nestin (*Nes*) levels were similar between Rax-
331 EGFP$^+$ and Rax-EGFP$^-$ cells (Fig. 3G–J). Levels of neither Darpp32 (*Ppp1r1b*) (71) nor Claudin1
332 (*Cldn1*), whose expression is restricted to the ventral part of tanycytes in the hypothalamus (72)
333 and other subventricular organs (73), showed differences between two groups. These results
334 implied that sorted Rax-EGFP$^+$ cells resembled the ventral part of tanycytes. In addition,
335 expression of *Dio2* and *Gpr50* was significantly increased in sorted Rax-EGFP$^+$ cells compared
336 with early hypothalamic progenitor cells (day 7 after hypothalamic differentiation from mESCs)
337 (Fig. 3K, L).
338
339 **Rax-EGFP$^+$ cells have a neurospherogenic potential**
340 In general, neural stem/progenitor cells dissociated into single cells form sphere-like
341 aggregates when cultured in serum-free medium containing growth factors such as FGF-2 and
342 EGF (74-76). These spheres are termed as “neurospheres”. Hypothalamic tanycytes have been

reported to form neurospheres (3,5,8), and their neurospherogenic potential differs between the ventral–dorsal locations of tanycytes (3). Therefore, we next examined the neurospherogenic ability of Rax-EGFP$^+$ cells. Rax-EGFP$^+$ cells cultured in DFNB medium supplemented with FGF-2, EGF, heparin, and CNTF (ciliary neurotrophic factor) (Fig. 4A) formed substantial numbers of neurospheres with coexpression of neural stem/progenitor cell markers (Fig. 4B–G). However, SOX2 expression within the Rax-EGFP$^+$ neurospheres was gradually reduced with every passage (Fig. 4B, D, F). Generally, CNTF, which promotes self-renewal and maintenance of neural stem cells (77,78), also has a stimulating effect on neurogenesis in the hypothalamus *in vivo* (79). We speculated that the reduction of SOX2 occurred because of the effect of CNTF.

Therefore, we attempted to form neurospheres without CNTF (Fig. 5A). Rax-EGFP$^+$ cells formed numerous neurospheres (Fig. 5B, C). These neurospheres expressed several typical neural stem/progenitor cell markers (Fig. 5D–G) including Bmi1, which is essential for the self-renewal of neural stem cells (80) (Fig. 5H). They also expressed Lhx2 (Fig. 5I) and BLBP (Fig. 5J) that are reported to be expressed in Fgf10$^+$ ventral tanycytes (4). The neurospheres showed diffuse BrdU incorporation (Fig. 5K) and a high proportion expressed Ki-67 (Fig. 5L). These results indicated the existence of proliferating neural stem/progenitor cells in neurospheres derived from Rax-EGFP$^+$ cells. FGFR1 was positive in the neurospheres (Fig. 5M), and phosphorylated Erk1/2 (pErk1/2), a common downstream signal, was detected (81) (Fig. 5N). In contrast to neurospheres

361 derived from dorsal α2-tanycytes (3), GFAP$^+$ or GLAST$^+$ cells were rarely present in Rax-EGFP$^+$
362 neurospheres (Fig. 5O, P).

363 Nkx2.1 is expressed in early progenitor cells of the ventral hypothalamus (82) (14) and in
364 tanycytes *in vivo* (83), while Pax6 is expressed in dorsal hypothalamic progenitors (14). The
365 neurospheres derived from Rax-EGFP$^+$ cells expressed Nkx2.1$^+$ in contrast to early progenitor
366 cells undergoing hypothalamic differentiation, which mainly expressed Pax6 (Fig. 6A–D).
367 Although a large proportion of Rax$^+$ cells among intermediate progenitors expressed Pax6
368 similarly to early progenitors, some Rax$^+$Nkx2.1$^+$ cells emerged (Fig. 6E, F). These data showed
369 that Rax-EGFP$^+$ cells sorted at the late stage of hypothalamic differentiation were different cell
370 types from early progenitors.

371 The neurospheres derived from Rax-EGFP$^+$ cells were stably passaged (every 5–7 days
372 for at least 10 passages), and even repeatedly passaged neurospheres expressed neural
373 stem/progenitor cell markers similarly to early passaged neurospheres (Fig. 7A–J). The mean
374 Sox2-positive rate throughout all passages was 75.6 ± 1.94% (mean ± s.e.m., n=9). In 5th passage
375 neurospheres, positive rates of vimentin and nestin were 69.3 ± 5.88% (mean ± s.e.m., n=6) and
376 66.7 ± 3.80% (mean ± s.e.m., n=5), respectively. All cells under neurosphere culture conditions
377 stably proliferated (Fig. 7K). They formed substantial numbers of neurospheres in each passage
378 (Fig. 7L).

These results showed that sorted Rax-EGFP$^+$ cells had high neurospherogenic potential.

Neurospheres derived from Rax-EGFP$^+$ cells are multipotent and differentiate into three neural lineages

Next, we analyzed the differentiation potential of neurospheres derived from Rax-EGFP$^+$ cells (Fig. 8A). When the neurospheres were attached to PDL-coated glass coverslips and cultured without FGF-2 or EGF, they differentiated into Tuj1$^+$ immature neurons (Fig. 8B–E), MAP2$^+$ NeuN$^+$ mature neurons (Fig. 8F), and GFAP$^+$ astrocytes (Fig. 8B-E). Early passaged neurospheres differentiated into NPY$^+$ hypothalamic neurons (Fig. 8G, H from 1st passage neurospheres), O4$^+$ Olig2$^+$ and CNPase$^+$ immature oligodendrocytes (Fig. 8I–K from 2nd passage neurospheres), and myelin basic protein (MBP)$^+$ Olig2$^+$ mature myelinating oligodendrocytes (84) (Fig. 8L from 2nd passage neurospheres). The proportion of NPY$^+$ neurons per Tuj1$^+$ neuron was 13.2 ± 1.56% (mean ± s.e.m., n=10). Some NPY$^+$ neurons coexpressed Rax, suggesting they were differentiated via Rax$^+$ cells (Fig. 8G, H). Furthermore, these neurospheres could be cryopreserved and retained the same differentiation abilities after thawing.

Consistently, neurospheres derived from Rax-EGFP$^+$ cells showed and maintained multipotency, differentiating into three neuronal lineages (neurons, astrocytes, and oligodendrocytes).

397

398 **FGF-2 is necessary for Rax-EGFP$^+$ cell proliferation and neurosphere formation**

399 In a previous report, FGF signaling was required for α-tanycyte proliferation *in vivo* and
400 *in vitro* (3). We found that the majority of Rax-EGFP$^+$ primary neurospheres were formed in the
401 absence of EGF as described previously (3). Therefore, FGF-2 might play a central role in
402 neurosphere formation from isolated Rax-EGFP$^+$ cells. We cultured Rax-EGFP$^+$ cells with or
403 without exogenous FGF-2 (Fig. 9A–D). In the absence of FGF-2, Rax-EGFP$^+$ cells rarely formed
404 neurospheres and were mainly floating as small aggregates expressing EGFP (Fig. 9C). The
405 number of neurospheres derived from Rax-EGFP$^+$ cells was significantly reduced in the non-FGF-
406 2 group (Fig. 9E).

407 We cultured Rax-EGFP$^+$ cells in the presence of the FGFR1 inhibitor SU5402 (3). The
408 formation of neurospheres cultured in medium containing FGF-2 and SU5402 was significantly
409 suppressed compared with medium containing FGF-2 alone, which was similar to the absence of
410 FGF-2 (Fig. 9F–J). Rax-EGFP$^+$ cells cultured with FGF-2 and SU5402 were floating as small
411 aggregates or single cells and rarely formed neurospheres. When they were transferred into
412 medium without SU5402, they formed some neurospheres (Fig. 9K, L). However, the expression
413 of EGFP was diminished in these reformed neurospheres.

414 These results showed that FGF-2 promotes the self-renewal of Rax-EGFP$^+$ cells and the

formation of neurospheres *in vitro*. Rax-EGFP$^+$ cells were responsive to FGF signaling similarly to tanycytes *in vivo*.

Neurospheres derived from Rax-EGFP$^+$ cells maintain the hypothalamic neural differentiation potential

We found that Rax expression in neurospheres was gradually reduced after passage 4–5, whereas Sox2 expression was preserved (Fig. 10A–J). We speculated that the long-term exposure of neurospheres to the high dose of exogenous FGF-2, which maintain neural stem cells in an undifferentiated state (85) and promotes self-renewal, might suppress their Rax expression. To evaluate this hypothesis, FGF-2-free medium was used to culture neurospheres (6th passage) that expressed low Rax but maintained FGFR1 expression (Fig. 10K). Although Rax$^+$ cells were almost entirely lost in the 6th passage of neurospheres (Fig. 10E), Rax expression was recovered by replacement with FGF-2-free differentiation medium along with hypothalamic differentiation in contrast to medium supplemented with FGF-2 (Fig. 10L–R). Furthermore, several cells that coexpressed Rax and Sox2 appeared among the differentiating cells (Fig. 10S, T).

Discussion

Rax is a characteristic marker of tanycytes in the adult hypothalamus (1,11). Of note, α2

433 and β tanycytes have been reported to highly express Rax compared with dorsal α1 tanycytes. Our
434 present study showed that Rax$^+$ cells preserved in the maturation phase of hypothalamic
435 differentiation from mESCs have a role as neural stem/progenitor cells similarly to tanycytes *in*
436 *vivo*. These cells were named "induced tanycyte-like cells" (iTan cells). They had similar
437 characteristics to ventral tanycytes with FGF signaling and substantial neurogenic abilities. This
438 is the first report of the induction and investigation of mESC-derived hypothalamic neural
439 stem/progenitor cells.

440 We confirmed that sorted Rax-EGFP$^+$ cells expressed neural stem/progenitor cell markers
441 such as SOX2, vimentin, nestin and Bmi1, which are also expressed by tanycytes. Rax-EGFP$^+$
442 cells differentiated into mature neurons and glial cells in 2D cultures similarly to tanycytes.
443 Furthermore, qRT-PCR analysis showed that Rax-EGFP$^+$ cells expressed *Fgf-10* and *Fgf-18* that
444 are expressed by vα2 tanycytes and β tanycytes (3,4,66). We also found relatively high *Lhx2*
445 expression in Rax-EGFP$^+$ cells. Several previous reports have shown *Lhx2* expression in the
446 embryonic hypothalamic neuroepithelium (16,86) and hypothalamic tanycytes (1,63). Lhx2 is
447 necessary to maintain *Rax* and tanycyte-specific genes, such as *Dio2* and *Gpr50*, in late progenitor
448 cells and tanycyte precursors during hypothalamus development (63). Rax-EGFP$^+$ cells highly
449 expressed *Dio2* and *Gpr50* compared with early hypothalamic progenitor cells. DIO2, which is
450 highly expressed in tanycytes, regulates the hypothalamus-pituitary-thyroid axis (68). Therefore,

451 Rax^+ iTan cells in the maturation phase of hypothalamic neural differentiation (days 22–25) are
452 considered to be different cell types from Rax^+ early hypothalamic progenitor cells (day 7). We
453 speculated that expression of Nkx2.1 might indicate the switching time from hypothalamic
454 progenitors to tanycytes. There were no $Rax^+Nkx2.1^+$ cells among early hypothalamic progenitors
455 in the culture condition without Shh treatment (14) in contrast to intermediate progenitors and
456 Rax^+ iTan cells. At least after day 13 when Otp^+Brn2^+ hypothalamic intermediate progenitors had
457 emerged (14), Rax^+ iTan cells might be differentiated in aggregates. Indeed, they were more
458 differentiated and similar to late progenitor cells and tanycytes. Some sorted Rax-$EGFP^+$ cells
459 differentiated into NPY^+ neurons that are reported to be generated from β tanycytes located in the
460 median eminence *in vivo* (1,4). These findings indicate that sorted Rax^+ iTan cells might resemble
461 ventral tanycytes (vα2 tanycytes or β tanycytes) that supply NPY neurons to the ARC *in vivo*.
462 Neurospheres were generated from cells derived from dorsal α2, α1, or vα2 tanycytes in
463 the presence of exogenous FGF-2, whereas no neurospheres were formed from β tanycytes (3). In
464 addition, α tanycytes proliferated in response to FGF ligands *in vivo* (3). In this study, we showed
465 that Rax^+ iTan cells formed substantial numbers of neurospheres that could be stably passaged.
466 BrdU analysis and Ki-67 immunostaining revealed that these Rax^+ iTan cells were highly
467 propagative. These neurospheres expressed representative neural stem/progenitor cell markers and
468 retained these markers when they were passaged repeatedly. Kawaguchi *et al* demonstrated that

469 highly nestin-expressing cells have both high multipotency and self-renewability (87). In the
470 present report, passaged neurospheres from Rax-EGFP$^+$ cells expressed nestin at about 66%,
471 indicating that our neurospheres were not homogenous. However, their relatively high purity,
472 which was shown by Sox2 expression in neurospheres, might be the result of cell sorting because
473 cells other than Rax$^+$ neural stem/progenitor cells, such as differentiated neurons and glial cells,
474 were excluded.

475 The requirement of FGF-2 signaling for the proliferation of Rax-EGFP$^+$ cells was
476 confirmed because FGFR1 inhibition prevented neurosphere formation by Rax-EGFP$^+$ cells. In
477 the hypothalamus, strong expression of the IIIc isoforms of FGFR1 and FGFR2 was observed,
478 which have a high affinity for FGF-2 (66,88). β Tanycytes also express FGFR1 and FGFR2 (6,89).
479 In the present study, we showed that Rax-EGFP$^+$ neurospheres diffusely expressed FGFR1. Taken
480 together, Rax$^+$ iTan cells propagate in response to exogenous FGF-2 through FGFR1.

481 The neuronal descendants of Fgf10$^+$ β tanycytes predominantly populate the ARC (4).
482 Moreover, β tanycytes that express *Rax* and *Lhx2*, as detected by *in situ* hybridization, give rise to
483 new neurons co-labeled with NPY or POMC (1). β Tanycytes are also reported to generate
484 astrocytes and oligodendrocyte precursor cells (1,2). However, GLAST$^+$ α tanycytes mainly
485 differentiate into astrocytes and their neurogenic potential was limited (3). This implies that β
486 tanycytes are more neurogenic, while α tanycytes are limited to be gliogenic (6). Neurospheres

487 derived from tanycytes *in vivo* are reported to differentiate into neurons and glial cells, such as
488 GHRH$^+$ hypothalamic neurons, GFAP$^+$ astrocytes and RIP$^+$ oligodendrocytes (3). In our present
489 report, neurospheres derived from Rax-EGFP$^+$ cells differentiated into three neuronal lineages,
490 mature neurons including hypothalamic NPY$^+$ neurons, GFAP$^+$ astrocytes, and MBP$^+$ Olig2$^+$
491 mature oligodendrocytes. These results showed that Rax$^+$ iTan cells *in vitro* appear to have
492 neuronal multipotency. However, Rax$^+$ iTan cells did not differentiate into POMC$^+$ neurons that
493 are differentiated from ventral tanycytes and have a crucial opposite effect to NPY$^+$ neurons on
494 food intake. In mice, the number of POMC$^+$ cells reaches a peak at E13.5, after which its
495 expression is extinguished as development progressed (90). Because we sorted Rax$^+$ iTan cells at
496 the very end of hypothalamic differentiation culture, we speculate that the culture condition might
497 need to be modified to promote the induction of POMC$^+$ neurons.

498 Rax expression in late passage neurospheres derived from Rax-EGFP$^+$ cells was reduced
499 by exposure to exogenous FGF-2, which had a central role in the maintenance of neural stem cells
500 in the SVZ and SGZ (91,92). Activation of FGFR1 and FGFR3 by FGF-2 promotes the self-
501 renewal of neural stem cells, whereas activation of other FGFRs promotes transition into different
502 subtypes of neural stem cells or their differentiation (93). In the present study, FGF-2 alone
503 appeared to be inadequate to maintain Rax expression in cell culture. We speculate that Rax
504 expression is sustained by the balance between self-renewal and differentiation signaling, which

might occur in tanycytes *in vivo*. However, passaged neurospheres derived from Rax-EGFP$^+$ cells (at least 6th passage) in the presence of FGF-2 differentiated into hypothalamic NPY$^+$ neurons and astrocytes regardless of their low Rax expression. Therefore, exogenous FGF-2 promotes self-renewal while maintaining the differentiation ability of Rax$^+$ iTan cells.

There are several limitations in this report. First, we did not compare Rax$^+$ iTan cells with tanycytes isolated from Rax-EGFP knock-in mice established from the mESCs used in this study, which would be a true comparable control. Second, *in vivo* transplantation experiments of Rax$^+$ iTan cells will be necessary to assess whether they can proliferate or differentiate into neuronal cells.

In summary, Rax$^+$ iTan cells remaining in the maturation phase of hypothalamic differentiation were considered to have the following properties. First, Rax$^+$ iTan cells functioned as neural stem/progenitor cells and had the ability to differentiate into three lines of neural cells, i.e. neurons (including hypothalamic neurons), astrocytes, and oligodendrocytes. Second, Rax$^+$ iTan cells resembled ventral tanycytes. Third, Rax$^+$ iTan cells self-renewed and formed neurospheres after exogenous FGF-2 addition. Neurospheres derived from Rax$^+$ iTan cells differentiated into hypothalamic neurons even when their Rax expression was suppressed by FGF-2.

These hypothalamic neural stem/progenitor cells may have many potential uses such as;

research tools to help develop the role of tanycytes for neurogenic potential or understand their metabolic functions, and in regenerative medicine of the hypothalamus. We have previously reported induction of dorsal hypothalamus from human ESCs (27). Our future studies will attempt to establish human tanycytes *in vitro*.

Acknowledgements

We are grateful to Hiroshi Kawasaki for detailed advice, Akira Mizoguchi for technical guidance regarding the perfusion of mice, Akane Yasui and Akiko Tsuzuki for technical assistances, and all members of the Arima laboratory for valuable discussions. We thank Mitchell Arico from Edanz Group (www.edanzediting.com/ac) for editing a draft of this manuscript.

Author Contributions

M.K., H.S., T.I and H.A. designed the project and wrote the manuscript. M.K., H.S and T.Y performed the experiments with technical assistance and advice from M.Sakakibara., M.Soen., H.O., K.M., T.K., M.Sugiyama, T.O., T.T., H.T., D.H., Y.I, S.I, M.G., and R.B.

Data Availability

The datasets generated during and/or analyzed during the current study are not publicly available

but are available from the corresponding author on reasonable request.

References

1. Lee DA, Bedont JL, Pak T, Wang H, Song J, Miranda-Angulo A, Takiar V, Charubhumi V, Balordi F, Takebayashi H, Aja S, Ford E, Fishell G, Blackshaw S. Tanycytes of the hypothalamic median eminence form a diet-responsive neurogenic niche. *Nat Neurosci*. 2012;15(5):700-702.

2. Lee DA, Blackshaw S. Functional implications of hypothalamic neurogenesis in the adult mammalian brain. *International journal of developmental neuroscience : the official journal of the International Society for Developmental Neuroscience*. 2012;30(8):615-621.

3. Robins SC, Stewart I, McNay DE, Taylor V, Giachino C, Goetz M, Ninkovic J, Briancon N, Maratos-Flier E, Flier JS, Kokoeva MV, Placzek M. alpha-Tanycytes of the adult hypothalamic third ventricle include distinct populations of FGF-responsive neural progenitors. *Nat Commun*. 2013;4:2049.

4. Haan N, Goodman T, Najdi-Samiei A, Stratford CM, Rice R, El Agha E, Bellusci S, Hajihosseini MK. Fgf10-expressing tanycytes add new neurons to the appetite/energy-balance regulating centers of the postnatal and adult hypothalamus. *J Neurosci*. 2013;33(14):6170-6180.

559 5. Zhang Y, Kim MS, Jia B, Yan J, Zuniga-Hertz JP, Han C, Cai D. Hypothalamic stem cells
560 control ageing speed partly through exosomal miRNAs. *Nature*. 2017;548(7665):52-57.
561 6. Goodman T, Hajihosseini MK. Hypothalamic tanycytes-masters and servants of metabolic,
562 neuroendocrine, and neurogenic functions. *Frontiers in neuroscience*. 2015;9:387.
563 7. Bolborea M, Dale N. Hypothalamic tanycytes: potential roles in the control of feeding and
564 energy balance. *Trends in neurosciences*. 2013;36(2):91-100.
565 8. Li J, Tang Y, Cai D. IKKbeta/NF-kappaB disrupts adult hypothalamic neural stem cells to
566 mediate a neurodegenerative mechanism of dietary obesity and pre-diabetes. *Nat Cell Biol*.
567 2012;14(10):999-1012.
568 9. Zoli M, Ferraguti F, Frasoldati A, Biagini G, Agnati LF. Age-related alterations in
569 tanycytes of the mediobasal hypothalamus of the male rat. *Neurobiol Aging*.
570 1995;16(1):77-83.
571 10. Rodriguez EM, Blazquez JL, Pastor FE, Pelaez B, Pena P, Peruzzo B, Amat P.
572 Hypothalamic tanycytes: a key component of brain-endocrine interaction. *Int Rev Cytol*.
573 2005;247:89-164.
574 11. Miranda-Angulo AL, Byerly MS, Mesa J, Wang H, Blackshaw S. Rax regulates
575 hypothalamic tanycyte differentiation and barrier function in mice. *J Comp Neurol*.
576 2014;522(4):876-899.

12. Prevot V, Dehouck B, Sharif A, Ciofi P, Giacobini P, Clasadonte J. The Versatile Tanycyte: A Hypothalamic Integrator of Reproduction and Energy Metabolism. *Endocr Rev*. 2018;39(3):333-368.

13. Furukawa T, Kozak CA, Cepko CL. rax, a novel paired-type homeobox gene, shows expression in the anterior neural fold and developing retina. *Proc Natl Acad Sci U S A*. 1997;94(7):3088-3093.

14. Wataya T, Ando S, Muguruma K, Ikeda H, Watanabe K, Eiraku M, Kawada M, Takahashi J, Hashimoto N, Sasai Y. Minimization of exogenous signals in ES cell culture induces rostral hypothalamic differentiation. *Proc Natl Acad Sci U S A*. 2008;105(33):11796-11801.

15. Eiraku M, Takata N, Ishibashi H, Kawada M, Sakakura E, Okuda S, Sekiguchi K, Adachi T, Sasai Y. Self-organizing optic-cup morphogenesis in three-dimensional culture. *Nature*. 2011;472(7341):51-56.

16. Shimogori T, Lee DA, Miranda-Angulo A, Yang Y, Wang H, Jiang L, Yoshida AC, Kataoka A, Mashiko H, Avetisyan M, Qi L, Qian J, Blackshaw S. A genomic atlas of mouse hypothalamic development. *Nat Neurosci*. 2010;13(6):767-775.

17. Pak T, Yoo S, Miranda-Angulo AL, Wang H, Blackshaw S. Rax-CreERT2 knock-in mice: a tool for selective and conditional gene deletion in progenitor cells and radial glia of the retina and hypothalamus. *PLoS One*. 2014;9(4):e90381.

595 18. Mathers PH, Grinberg A, Mahon KA, Jamrich M. The Rx homeobox gene is essential for
596 vertebrate eye development. *Nature*. 1997;387(6633):603-607.
597 19. Lu F, Kar D, Gruenig N, Zhang ZW, Cousins N, Rodgers HM, Swindell EC, Jamrich M,
598 Schuurmans C, Mathers PH, Kurrasch DM. Rax is a selector gene for mediobasal
599 hypothalamic cell types. *J Neurosci*. 2013;33(1):259-272.
600 20. Altman J, Bayer SA. Development of the diencephalon in the rat. III. Ontogeny of the
601 specialized ventricular linings of the hypothalamic third ventricle. *J Comp Neurol*.
602 1978;182(4 Pt 2):995-1015.
603 21. Rutzel H, Schiebler TH. Prenatal and early postnatal development of the glial cells in the
604 median eminence of the rat. *Cell Tissue Res*. 1980;211(1):117-137.
605 22. Watanabe K, Kamiya D, Nishiyama A, Katayama T, Nozaki S, Kawasaki H, Watanabe Y,
606 Mizuseki K, Sasai Y. Directed differentiation of telencephalic precursors from embryonic
607 stem cells. *Nat Neurosci*. 2005;8(3):288-296.
608 23. Sasai Y, Eiraku M, Suga H. In vitro organogenesis in three dimensions: self-organising
609 stem cells. *Development*. 2012;139(22):4111-4121.
610 24. Suga H, Kadoshima T, Minaguchi M, Ohgushi M, Soen M, Nakano T, Takata N, Wataya T,
611 Muguruma K, Miyoshi H, Yonemura S, Oiso Y, Sasai Y. Self-formation of functional
612 adenohypophysis in three-dimensional culture. *Nature*. 2011;480(7375):57-62.

613 25. Ozone C, Suga H, Eiraku M, Kadoshima T, Yonemura S, Takata N, Oiso Y, Tsuji T, Sasai
614 Y. Functional anterior pituitary generated in self-organizing culture of human embryonic
615 stem cells. *Nat Commun*. 2016;7:10351.
616 26. Merkle FT, Maroof A, Wataya T, Sasai Y, Studer L, Eggan K, Schier AF. Generation of
617 neuropeptidergic hypothalamic neurons from human pluripotent stem cells. *Development*.
618 2015;142(4):633-643.
619 27. Ogawa K, Suga H, Ozone C, Sakakibara M, Yamada T, Kano M, Mitsumoto K, Kasai T,
620 Kodani Y, Nagasaki H, Yamamoto N, Hagiwara D, Goto M, Banno R, Sugimura Y, Arima
621 H. Vasopressin-secreting neurons derived from human embryonic stem cells through
622 specific induction of dorsal hypothalamic progenitors. *Sci Rep*. 2018;8(1):3615.
623 28. Wang L, Meece K, Williams DJ, Lo KA, Zimmer M, Heinrich G, Martin Carli J, Leduc
624 CA, Sun L, Zeltser LM, Freeby M, Goland R, Tsang SH, Wardlaw SL, Egli D, Leibel RL.
625 Differentiation of hypothalamic-like neurons from human pluripotent stem cells. *J Clin*
626 *Invest*. 2015;125(2):796-808.
627 29. Kawasaki H, Mizuseki K, Nishikawa S, Kaneko S, Kuwana Y, Nakanishi S, Nishikawa SI,
628 Sasai Y. Induction of midbrain dopaminergic neurons from ES cells by stromal cell-derived
629 inducing activity. *Neuron*. 2000;28(1):31-40.
630 30. RRID:SCR_016979, https://scicrunch.org/resolver/SCR_016979.

631 31. RRID:SCR_003070, https://scicrunch.org/resolver/SCR_003070.

632 32. RRID:AB_2313978, https://scicrunch.org/resolver/AB_2313978.

633 33. RRID:AB_880078, https://scicrunch.org/resolver/AB_880078.

634 34. RRID:AB_2065390, https://scicrunch.org/resolver/AB_2065390.

635 35. RRID:AB_626766, https://scicrunch.org/resolver/AB_626766.

636 36. RRID:AB_2082593, https://scicrunch.org/resolver/AB_2082593.

637 37. RRID:AB_2315112, https://scicrunch.org/resolver/AB_2315112.

638 38. RRID:AB_11178519, https://scicrunch.org/resolver/AB_11178519.

639 39. RRID:AB_10013361, https://scicrunch.org/resolver/AB_10013361.

640 40. RRID:AB_2109645, https://scicrunch.org/resolver/AB_2109645.

641 41. RRID:AB_304334, https://scicrunch.org/resolver/AB_304334.

642 42. RRID:AB_442102, https://scicrunch.org/resolver/AB_442102.

643 43. RRID:AB_2783558, https://scicrunch.org/resolver/AB_2783558.

644 44. RRID:AB_2138153, https://scicrunch.org/resolver/AB_2138153.

645 45. RRID:AB_94975, https://scicrunch.org/resolver/AB_94975.

646 46. RRID:AB_10094393, https://scicrunch.org/resolver/AB_10094393.

647 47. RRID:AB_2298772, https://scicrunch.org/resolver/AB_2298772.

648 48. RRID:AB_86728, https://scicrunch.org/resolver/AB_86728.

649 49. RRID:AB_2716286, https://scicrunch.org/resolver/AB_2716286.

650 50. RRID:AB_11213138, https://scicrunch.org/resolver/AB_11213138.

651 51. RRID:AB_570666, https://scicrunch.org/resolver/AB_570666.

652 52. RRID:AB_291612, https://scicrunch.org/resolver/AB_291612.

653 53. RRID:AB_2307442, https://scicrunch.org/resolver/AB_2307442.

654 54. RRID:AB_2783560, https://scicrunch.org/resolver/AB_2783560.

655 55. RRID:AB_2783559, https://scicrunch.org/resolver/AB_2783559.

656 56. RRID:AB_1623028, https://scicrunch.org/resolver/AB_1623028.

657 57. RRID:AB_2313773, https://scicrunch.org/resolver/AB_2313773.

658 58. RRID:AB_11212377, https://scicrunch.org/resolver/AB_11212377.

659 59. RRID:SCR_016264, https://scicrunch.org/resolver/SCR_016264.

660 60. RRID:SCR_016980, https://scicrunch.org/resolver/SCR_016980.

661 61. RRID:SCR_014199, https://scicrunch.org/resolver/SCR_014199.

662 62. RRID:SCR_002865, https://scicrunch.org/resolver/SCR_002865.

663 63. Salvatierra J, Lee DA, Zibetti C, Duran-Moreno M, Yoo S, Newman EA, Wang H, Bedont
664 JL, de Melo J, Miranda-Angulo AL, Gil-Perotin S, Garcia-Verdugo JM, Blackshaw S. The
665 LIM homeodomain factor Lhx2 is required for hypothalamic tanycyte specification and
666 differentiation. *J Neurosci*. 2014;34(50):16809-16820.

667 64. Izant JG, McIntosh JR. Microtubule-associated proteins: a monoclonal antibody to MAP2
668 binds to differentiated neurons. *Proc Natl Acad Sci U S A*. 1980;77(8):4741-4745.
669 65. Bignami A, Eng LF, Dahl D, Uyeda CT. Localization of the glial fibrillary acidic protein
670 in astrocytes by immunofluorescence. *Brain research*. 1972;43(2):429-435.
671 66. Hajihosseini MK, De Langhe S, Lana-Elola E, Morrison H, Sparshott N, Kelly R, Sharpe
672 J, Rice D, Bellusci S. Localization and fate of Fgf10-expressing cells in the adult mouse
673 brain implicate Fgf10 in control of neurogenesis. *Molecular and cellular neurosciences*.
674 2008;37(4):857-868.
675 67. de Vries EM, Kwakkel J, Eggels L, Kalsbeek A, Barrett P, Fliers E, Boelen A. NFkappaB
676 signaling is essential for the lipopolysaccharide-induced increase of type 2 deiodinase in
677 tanycytes. *Endocrinology*. 2014;155(5):2000-2008.
678 68. Fekete C, Lechan RM. Central regulation of hypothalamic-pituitary-thyroid axis under
679 physiological and pathophysiological conditions. *Endocr Rev*. 2014;35(2):159-194.
680 69. Muller-Fielitz H, Stahr M, Bernau M, Richter M, Abele S, Krajka V, Benzin A, Wenzel J,
681 Kalies K, Mittag J, Heuer H, Offermanns S, Schwaninger M. Tanycytes control the
682 hormonal output of the hypothalamic-pituitary-thyroid axis. *Nat Commun*. 2017;8(1):484.
683 70. Batailler M, Mullier A, Sidibe A, Delagrange P, Prevot V, Jockers R, Migaud M.
684 Neuroanatomical distribution of the orphan GPR50 receptor in adult sheep and rodent

brains. *Journal of neuroendocrinology*. 2012;24(5):798-808.

71. Meister B, Hokfelt T, Tsuruo Y, Hemmings H, Ouimet C, Greengard P, Goldstein M. DARPP-32, a dopamine- and cyclic AMP-regulated phosphoprotein in tanycytes of the mediobasal hypothalamus: distribution and relation to dopamine and luteinizing hormone-releasing hormone neurons and other glial elements. *Neuroscience*. 1988;27(2):607-622.

72. Mullier A, Bouret SG, Prevot V, Dehouck B. Differential distribution of tight junction proteins suggests a role for tanycytes in blood-hypothalamus barrier regulation in the adult mouse brain. *J Comp Neurol*. 2010;518(7):943-962.

73. Langlet F, Mullier A, Bouret SG, Prevot V, Dehouck B. Tanycyte-like cells form a blood-cerebrospinal fluid barrier in the circumventricular organs of the mouse brain. *J Comp Neurol*. 2013;521(15):3389-3405.

74. Laywell ED, Rakic P, Kukekov VG, Holland EC, Steindler DA. Identification of a multipotent astrocytic stem cell in the immature and adult mouse brain. *Proc Natl Acad Sci U S A*. 2000;97(25):13883-13888.

75. Reynolds BA, Weiss S. Generation of neurons and astrocytes from isolated cells of the adult mammalian central nervous system. *Science*. 1992;255(5052):1707-1710.

76. Reynolds BA, Tetzlaff W, Weiss S. A multipotent EGF-responsive striatal embryonic progenitor cell produces neurons and astrocytes. *J Neurosci*. 1992;12(11):4565-4574.

703 77. Bauer S, Kerr BJ, Patterson PH. The neuropoietic cytokine family in development,
704 plasticity, disease and injury. *Nature reviews Neuroscience*. 2007;8(3):221-232.
705 78. Shimazaki T, Shingo T, Weiss S. The ciliary neurotrophic factor/leukemia inhibitory
706 factor/gp130 receptor complex operates in the maintenance of mammalian forebrain neural
707 stem cells. *J Neurosci*. 2001;21(19):7642-7653.
708 79. Kokoeva MV, Yin H, Flier JS. Neurogenesis in the hypothalamus of adult mice: potential
709 role in energy balance. *Science*. 2005;310(5748):679-683.
710 80. Molofsky AV, Pardal R, Iwashita T, Park IK, Clarke MF, Morrison SJ. Bmi-1 dependence
711 distinguishes neural stem cell self-renewal from progenitor proliferation. *Nature*.
712 2003;425(6961):962-967.
713 81. Mason I. Initiation to end point: the multiple roles of fibroblast growth factors in neural
714 development. *Nature reviews Neuroscience*. 2007;8(8):583-596.
715 82. Marin O, Baker J, Puelles L, Rubenstein JL. Patterning of the basal telencephalon and
716 hypothalamus is essential for guidance of cortical projections. *Development*.
717 2002;129(3):761-773.
718 83. Yee CL, Wang Y, Anderson S, Ekker M, Rubenstein JL. Arcuate nucleus expression of
719 NKX2.1 and DLX and lineages expressing these transcription factors in neuropeptide Y(+),
720 proopiomelanocortin(+), and tyrosine hydroxylase(+) neurons in neonatal and adult mice.

721 *J Comp Neurol*. 2009;517(1):37-50.

722 84. Nishiyama A, Komitova M, Suzuki R, Zhu X. Polydendrocytes (NG2 cells):
723 multifunctional cells with lineage plasticity. *Nature reviews Neuroscience*. 2009;10(1):9-
724 22.

725 85. Faux CH, Turnley AM, Epa R, Cappai R, Bartlett PF. Interactions between fibroblast
726 growth factors and Notch regulate neuronal differentiation. *J Neurosci*. 2001;21(15):5587-
727 5596.

728 86. Roy A, de Melo J, Chaturvedi D, Thein T, Cabrera-Socorro A, Houart C, Meyer G,
729 Blackshaw S, Tole S. LHX2 is necessary for the maintenance of optic identity and for the
730 progression of optic morphogenesis. *J Neurosci*. 2013;33(16):6877-6884.

731 87. Kawaguchi A, Miyata T, Sawamoto K, Takashita N, Murayama A, Akamatsu W, Ogawa
732 M, Okabe M, Tano Y, Goldman SA, Okano H. Nestin-EGFP transgenic mice: visualization
733 of the self-renewal and multipotency of CNS stem cells. *Molecular and cellular*
734 *neurosciences*. 2001;17(2):259-273.

735 88. Zhang X, Ibrahimi OA, Olsen SK, Umemori H, Mohammadi M, Ornitz DM. Receptor
736 specificity of the fibroblast growth factor family. The complete mammalian FGF family. *J*
737 *Biol Chem*. 2006;281(23):15694-15700.

738 89. Belluardo N, Wu G, Mudo G, Hansson AC, Pettersson R, Fuxe K. Comparative localization

739 of fibroblast growth factor receptor-1, -2, and -3 mRNAs in the rat brain: in situ
740 hybridization analysis. *J Comp Neurol*. 1997;379(2):226-246.
741 90. Padilla SL, Carmody JS, Zeltser LM. Pomc-expressing progenitors give rise to antagonistic
742 neuronal populations in hypothalamic feeding circuits. *Nat Med*. 2010;16(4):403-405.
743 91. Sanai N, Tramontin AD, Quinones-Hinojosa A, Barbaro NM, Gupta N, Kunwar S, Lawton
744 MT, McDermott MW, Parsa AT, Manuel-Garcia Verdugo J, Berger MS, Alvarez-Buylla A.
745 Unique astrocyte ribbon in adult human brain contains neural stem cells but lacks chain
746 migration. *Nature*. 2004;427(6976):740-744.
747 92. Galvez-Contreras AY, Gonzalez-Castaneda RE, Luquin S, Gonzalez-Perez O. Role of
748 fibroblast growth factor receptors in astrocytic stem cells. *Current signal transduction*
749 *therapy*. 2012;7(1):81-86.
750 93. Maric D, Fiorio Pla A, Chang YH, Barker JL. Self-renewing and differentiating properties
751 of cortical neural stem cells are selectively regulated by basic fibroblast growth factor
752 (FGF) signaling via specific FGF receptors. *J Neurosci*. 2007;27(8):1836-1852.

753

754 **Legends**

755 **Figure 1. Rax-EGFP^{+} cells are sustained in the maturation phase of hypothalamic**
756 **differentiation.**

A) Coronal section of the adult hypothalamus from a male C57BL/6 mouse (2 months old). Tanycytes are divided into four subtypes (α1, dorsal α2, ventral α2, β tanycytes).

B–E) Hypothalamic sections from a male C57BL/6 mouse (2 months old) were immunostained for Rax (B, red), Sox2 (C, red), vimentin (D, red), and nestin (E, red).

F) Schematic of the culture protocol for hypothalamic differentiation from mESCs. Rax-EGFP^{+} and Rax-EGFP^{-} cells were sorted by FACS on days 22–25.

G) Immunostaining of early hypothalamic progenitor cells. The peak expression of Rax-EGFP on day 7 in the hypothalamic differentiation. Rax (magenta) and Rax::EGFP (green).

H–J) In the maturation phase of hypothalamic differentiation, various hypothalamic neurons were observed. Aggregates in Millicell inserts are shown. AVP (H, red), NPY (I, red), and POMC (J, red).

K) Some cells expressed Rax-EGFP in the maturation phase of hypothalamic differentiation. GFAP (magenta), Rax::EGFP (green), and Tuj1 (yellow).

L, M) High magnification images of the Rax-EGFP^{+} area. Some Rax-EGFP^{+} cells had process-like structures (M, white arrowhead). Rax::EGFP (green). For all relevant panels, nuclear counterstaining was performed with DAPI (blue). Scale bars: 100 μm (B–E, K); 50 μm (G, L); 20 μm (H–J, M).

775 **Table 1. Cell markers for hypothalamic tanycytes.**

776 Rax is strongly expressed in α2 and β tanycytes.

777

778 **Figure 2. Sorted Rax-EGFP$^+$ cells express neural stem/progenitor markers and differentiate**

779 **into neurons and astrocytes.**

780 A–C) Immunostaining of Rax-EGFP$^+$ cells for GFP (A) and Rax (B), and a merged image (C).

781 Rax (B and C, magenta) and Rax::EGFP (A and C, green).

782 D–G) Rax-EGFP$^+$ cells expressed representative neural stem/progenitor cell markers including

783 Sox2 (D, E), vimentin (F), and nestin (G). Sox2 (D, E, green), Rax (E, magenta), vimentin (F,

784 magenta), and nestin (G, yellow).

785 H) Rax-EGFP$^+$ cells expressed Lhx2, a ventral tanycyte marker. Lhx2 (H, red).

786 I–K) Immunostaining of differentiated Rax-EGFP$^+$ cells on PDL-coated glass coverslips on day 5.

787 Rax-GFP$^+$ cells directly differentiated into mature hypothalamic neurons and astrocytes. MAP2 (I,

788 magenta), NeuN (I, green), GFAP (J, magenta), NPY (K, magenta), and Tuj1 (J and K, green). For

789 all relevant panels, nuclear counterstaining was performed with DAPI (blue). Scale bars: 20 μm.

790

791 **Figure 3. Rax-EGFP$^+$ cells express ventral tanycyte markers including FGF.**

792 A–J) qPCR analysis of Rax-EGFP$^+$ and Rax-EGFP$^-$ cells. Relative mRNA expression levels of

793 *Rax* (A), *Fgf-10* (B), *Fgf-18* (C), *Lhx2* (D), *Dio2* (E), and *Gpr50* (F) were significantly increased

794 in Rax-EGFP$^+$ cells. There was no significant difference in *Vim* (G), *Nes* (H), *Ppp1r1b* (I), or *Cldn1*

795 (J) expression between the two groups. n=5 (A–D, G–J), 9 (E) and 10 (F).

796 K, L) qPCR analysis of Rax-EGFP$^+$ and early hypothalamic progenitor cells. Relative mRNA

797 expression levels of *Dio2* (K) and *Gpr50* (L) were significantly increased in Rax-EGFP$^+$ cells. n=5.

798 Mean ± S.E.M. *P<0.05, **P < 0.01.

799

800 **Figure 4. Rax-EGFP$^+$ neurosphere culture in medium supplemented with CNTF.**

801 A) Culture protocol for neurospheres derived from Rax-EGFP$^+$ cells.

802 B–G) Rax-EGFP$^+$ neurospheres cultured in medium supplemented with CNTF. SOX2 expression

803 within the neurospheres was gradually reduced with each passage. Rax (B, D, F, magenta), Sox2

804 (B, D, F, green), vimentin (C, E, G, magenta), and nestin (C, E, G, yellow). For all relevant panels,

805 nuclear counterstaining was performed with DAPI (blue). Scale bars: 50 μm.

806

807 **Figure 5. Rax-EGFP$^+$ cells have a neurospherogenic potential.**

808 A) Culture protocol for neurospheres derived from Rax-EGFP$^+$ cells. Pink spheres indicate Rax$^+$

809 neural stem/progenitor cells. Blue spheres indicate other cells.

810 B, C) Rax-EGFP$^+$ cells formed substantial numbers of neurospheres. Fluorescence (B) and phase

811 contrast microscopy images (C). Rax::EGFP (B, green).

812 D–H) Immunostaining of 1st passage neurospheres derived from Rax-EGFP$^+$ cells. Cells within

813 neurospheres abundantly expressed neural stem/progenitor cell markers. Rax (D and F, magenta),

814 Sox2 (E and F, green), vimentin (G, magenta), nestin (G yellow), and Bmi1 (H, red).

815 I–L) 1st passage neurospheres expressed Lhx2 and BLBP similarly to ventral tanycytes (I, J).

816 Neurospheres showed high BrdU incorporation (K). Ki-67$^+$ cells were observed throughout the

817 neurospheres (L). Lhx2 (I, red), BLBP (J, red), BrdU (K, red), Rax (L, magenta), and Ki-67 (L,

818 green).

819 M, N) Cells showed FGFR1 and pErk1/2 expression, although pErk1/2 was limited to the surface

820 of 1st passage neurospheres. FGFR1 (M, red), and pErk1/2 (N, red).

821 O, P) There were very few GFAP$^+$ or GLAST$^+$ cells in neurospheres. GFAP (O, red) and GLAST

822 (P, red). For all relevant panels, nuclear counterstaining was performed with DAPI (blue). Scale

823 bars: 100 μm (B, C); 50 μm (D–P).

824

825 **Figure 6. Comparison between Rax-EGFP$^+$ neurospheres and hypothalamic progenitors**

826 **derived from mESCs.**

827 A–F) Comparison of 1st passage neurospheres derived from Rax-EGFP$^+$ cells and two stage

828 hypothalamic progenitors. The 1st passage neurospheres showed high Nkx2.1 and low Pax6

829 expression in contrast to early progenitor cells. However, some $Rax^{+}Nkx2.1^{+}$ cells ware observed
830 among intermediate progenitor cells. Rax (A, C, E, magenta), Nkx2.1 (A, C, E, green), Pax6 (B,
831 D, F, magenta), and Rax::EGFP (B, D, F, green). For all relevant panels, nuclear counterstaining
832 was performed with DAPI (blue). Scale bars: 50 μm.
833
834 **Figure 7. Neurospheres derived from Rax-$EGFP^{+}$ cells can be stably passaged.**
835 A–I) Neurospheres derived from Rax-$EGFP^{+}$ cells were passaged stably. Repeatedly passaged
836 neurospheres extensively expressed neural stem/progenitor cell markers similar to early passage
837 neurospheres. 2nd passage (A–C), 6th passage (D–F), and 9th passage (G–I). Sox2 (A, D, G, white),
838 vimentin (B, E, H, magenta), nestin (C, F, I, yellow), and DAPI (A, D, G, blue). Scale bars: 50 μm.
839 J) Sox2-positive rate of neurospheres derived from Rax-$EGFP^{+}$ cells, n=5 per group.
840 K) Growth rate of all cells under neurosphere culture conditions, n=2.
841 L) Number of neurospheres in each passage (1st to 5th passage), n=5 per group.
842
843 **Figure 8. Neurospheres derived from Rax-$EGFP^{+}$ cells are multipotent and differentiate into**
844 **three neural lineages.**
845 A) Culture protocol for neurosphere differentiation.
846 B–E) Neurospheres derived from Rax-$EGFP^{+}$ cells differentiated into $Tuj1^{+}$ immature neurons and

847 GFAP$^+$ astrocytes. 1st passage (B), 2nd passage (C), 3rd passage (D), and 4th passage (E). GFAP

848 (magenta), and Tuj1 (yellow).

849 F–L) Neurospheres derived from Rax-EGFP$^+$ cells differentiated into three neural lineages: mature

850 neurons (some were NPY$^+$), astroctyes, and immature and mature oligodendrocytes. The NPY$^+$

851 neuron in (H) had long complex neurites. MAP2 (F, magenta), NeuN (F, green), NPY (G and H,

852 magenta), Rax (G and H, green), O4 (I and J, magenta), Tuj1 (I, green), Olig2 (J and L, green),

853 CNPase (K, red), and MBP (L, magenta). For all relevant panels, nuclear counterstaining was

854 performed with DAPI (blue). Scale bars: 100 μm (B–E); 50 μm (F–L).

855

856 **Figure 9. FGF-2 is necessary for the formation of neurospheres derived from Rax-EGFP$^+$**

857 **cells.**

858 A–D) Phase contrast and fluorescence microscopy images of Rax-EGFP$^+$ cells cultured with or

859 without FGF-2. Rax::EGFP (green).

860 E) Numbers of neurospheres per well were significantly reduced in the non-FGF-2 group. n=5.

861 Mean ± S.E.M. **P < 0.01.

862 F–I) Merged images of Rax-EGFP$^+$ neurospheres on day 5. Rax::EGFP (green).

863 J) Numbers of neurospheres per well were significantly reduced for Rax-EGFP$^+$ cells cultured in

864 medium containing FGF-2 and SU5402. n=5 each group. Mean ± S.E.M. *P < 0.05.

K) No neurospheres were observed when Rax-EGFP$^+$ cells were cultured with FGF-2 + SU5402.

L) When cells were transferred into fresh medium with FGF-2, some newly generated neurospheres were observed. Scale bars: 100 μm (A–D); 50 μm (K, L).

Figure 10. Exogenous FGF-2 suppresses Rax expression in neurospheres.

A–J) Rax expression within neurospheres derived from Rax-EGFP$^+$ cells was reduced after the 4th passage (A–E), whereas Sox2 expression was preserved in late passage neurospheres (F–J). Rax expression disappeared in a high proportion of 6th passage neurospheres. Rax (A–E, red), and Sox (F–J, white).

K) Culture protocol for the differentiation of 6th passage neurospheres. The 6th passage neurospheres were cultured as floating aggregates in two groups: DFNB + FGF-2 and DFNB alone.

L–Q) 6th passage neurospheres cultured without FGF-2 differentiated into NPY$^+$ neurons and glial cells. Rax expression was observed in some cells. Rax (L and O, red), GFAP (M and P, magenta), Tuj1 (M and P, green), NPY (N and Q, red), and Rax (N and Q, green).

R) Rax-positive rate of 6th passage neurospheres cultured in DFNB with/without FGF-2. n=9. Mean ± S.E.M. **P < 0.01.

S, T) Some 6th passage neurospheres cultured in DFNB without FGF-2 expressed Rax and SOX2. Rax (magenta) and Sox2 (green). For all relevant panels, nuclear counterstaining was performed

883 with DAPI (blue). Scale bars: 50 μm.

Table 1

	α1 tanycytes	Dorsal α2-tanycytes	Ventral α2-tanycytes	β tanycytes
Sox2	+	+	+	+
Vimentin	+	+	+	++
Nestin	+	+	+	++
Bmi1	+	+	+	+
Rax	+	++	++	++
Lhx2	-	-	+	++
Fgf-10	-	-	+	+
Fgf-18	-	-	+	-
GFAP	+	+	-	-

Figure 1

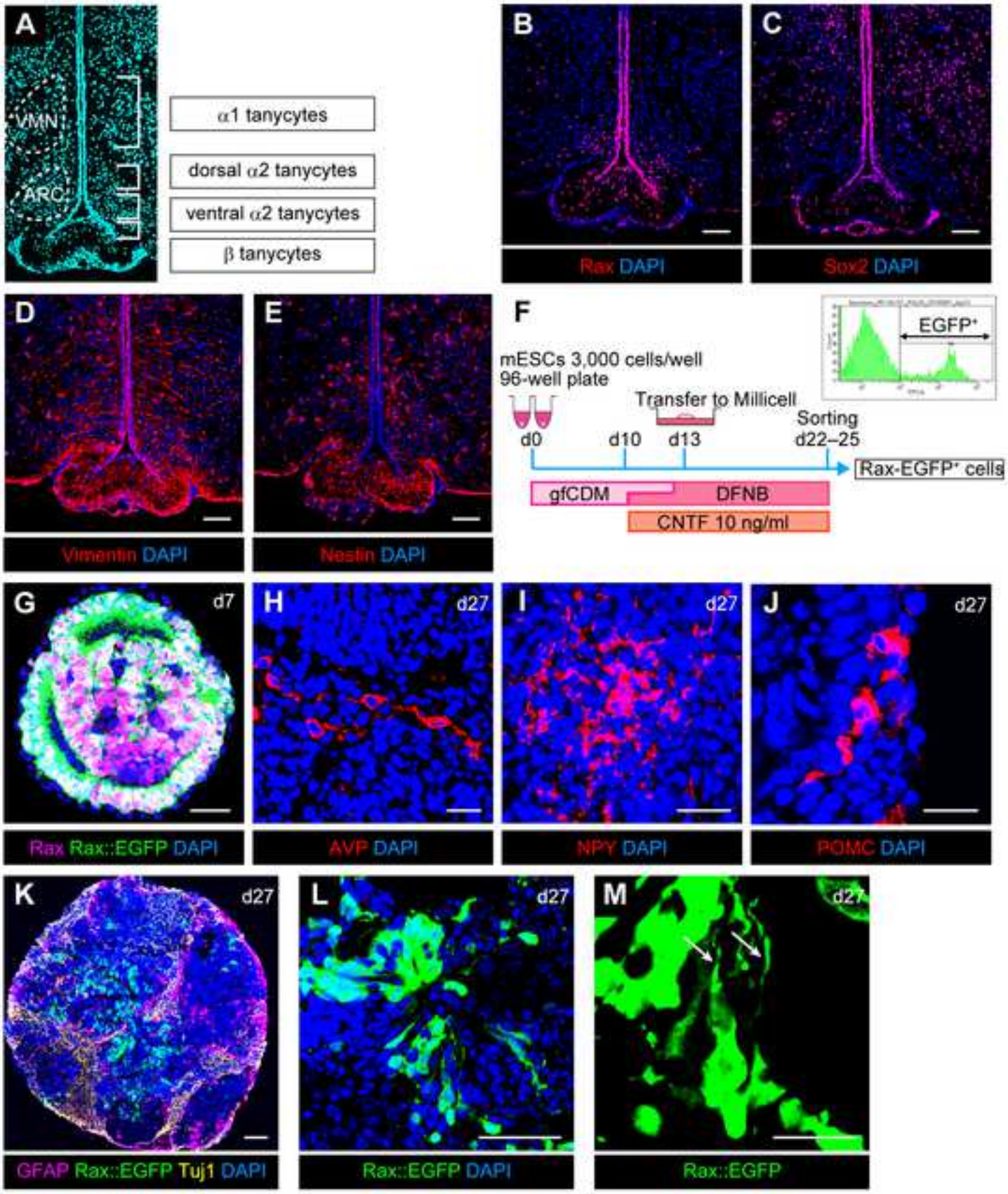
A
VMN
ARC
α1 tanycytes
dorsal α2 tanycytes
ventral α2 tanycytes
β tanycytes
B
Rax DAPI
C
Sox2 DAPI
D
Vimentin DAPI
E
Nestin DAPI
F
mESCs 3,000 cells/well
96-well plate
Transfer to Millicell
Sorting
d0
d10
d13
d22–25
Rax-EGFP⁺ cells
gfCDM
DFNB
CNTF 10 ng/ml
EGFP⁺
G
d7
Rax Rax::EGFP DAPI
H
d27
AVP DAPI
I
d27
NPY DAPI
J
d27
POMC DAPI
K
d27
GFAP Rax::EGFP Tuj1 DAPI
L
d27
Rax::EGFP DAPI
M
d27
Rax::EGFP

Figure 2

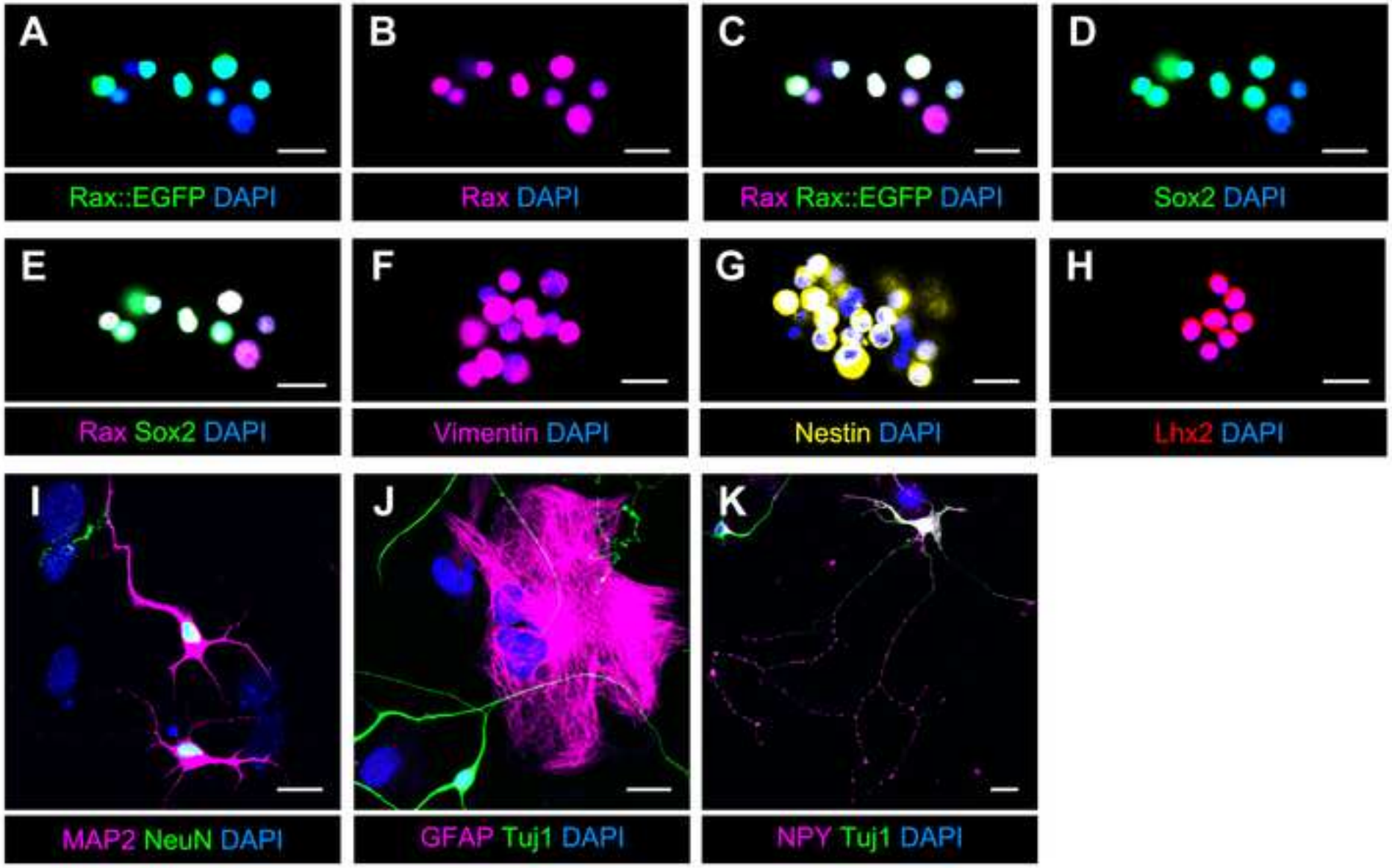
A
Rax::EGFP DAPI
B
Rax DAPI
C
Rax Rax::EGFP DAPI
D
Sox2 DAPI
E
Rax Sox2 DAPI
F
Vimentin DAPI
G
Nestin DAPI
H
Lhx2 DAPI
I
MAP2 NeuN DAPI
J
GFAP Tuj1 DAPI
K
NPY Tuj1 DAPI

Figure 3

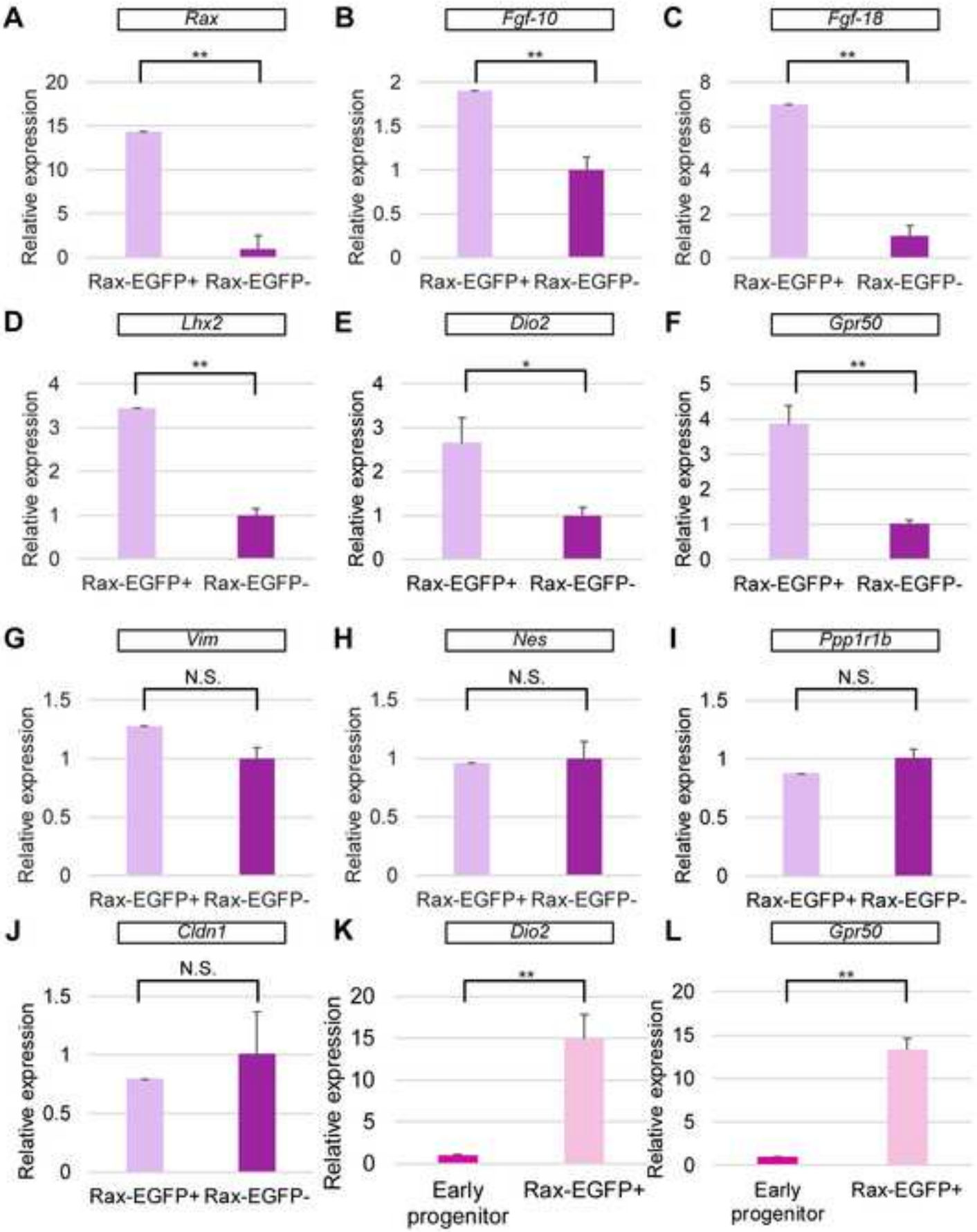
A
Rax
**
Relative expression
20
15
10
5
0
Rax-EGFP+
Rax-EGFP-
B
Fgf-10
**
Relative expression
2
1.5
1
0.5
0
Rax-EGFP+
Rax-EGFP-
C
Fgf-18
**
Relative expression
8
6
4
2
0
Rax-EGFP+
Rax-EGFP-
D
Lhx2
**
Relative expression
4
3
2
1
0
Rax-EGFP+
Rax-EGFP-
E
Dio2
*
Relative expression
4
3
2
1
0
Rax-EGFP+
Rax-EGFP-
F
Gpr50
**
Relative expression
5
4
3
2
1
0
Rax-EGFP+
Rax-EGFP-
G
Vim
N.S.
Relative expression
1.5
1
0.5
0
Rax-EGFP+
Rax-EGFP-
H
Nes
N.S.
Relative expression
1.5
1
0.5
0
Rax-EGFP+
Rax-EGFP-
I
Ppp1r1b
N.S.
Relative expression
1.5
1
0.5
0
Rax-EGFP+
Rax-EGFP-
J
Cldn1
N.S.
Relative expression
1.5
1
0.5
0
Rax-EGFP+
Rax-EGFP-
K
Dio2
**
Relative expression
20
15
10
5
0
Early progenitor
Rax-EGFP+
L
Gpr50
**
Relative expression
20
15
10
5
0
Early progenitor
Rax-EGFP+

Figure 4

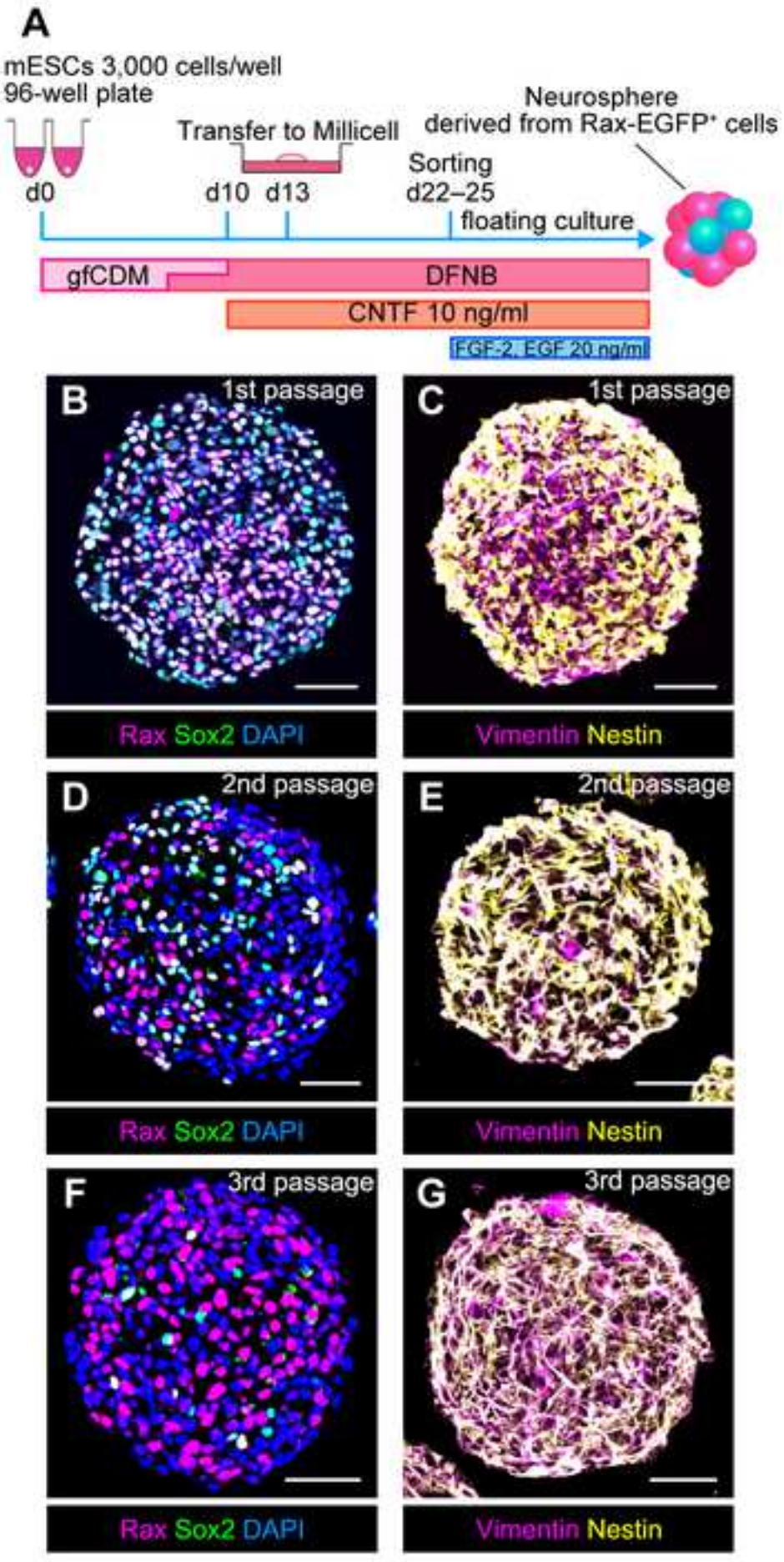
A
mESCs 3,000 cells/well
96-well plate
Transfer to Millicell
Neurosphere
derived from Rax-EGFP+ cells
Sorting
d22–25
d0
d10 d13
floating culture
gfCDM
DFNB
CNTF 10 ng/ml
FGF-2, EGF 20 ng/ml
B
1st passage
Rax Sox2 DAPI
C
1st passage
Vimentin Nestin
D
2nd passage
Rax Sox2 DAPI
E
2nd passage
Vimentin Nestin
F
3rd passage
Rax Sox2 DAPI
G
3rd passage
Vimentin Nestin

Figure 5

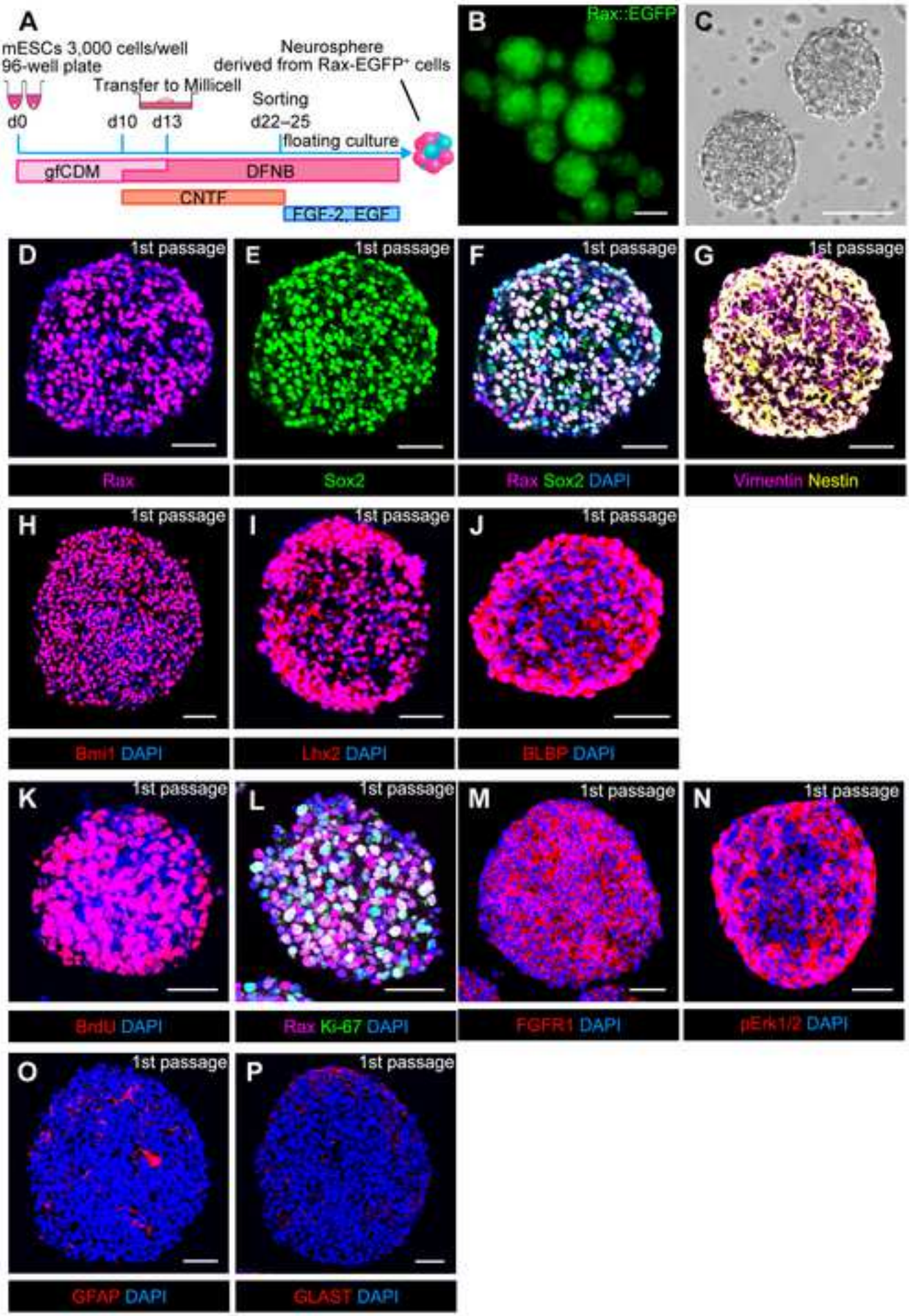
A
mESCs 3,000 cells/well
96-well plate
Transfer to Millicell
Neurosphere
derived from Rax-EGFP+ cells
Sorting
d0
d10
d13
d22–25
floating culture
gfCDM
DFNB
CNTF
FGF-2 EGF
B
Rax::EGFP
C
D
1st passage
Rax
E
1st passage
Sox2
F
1st passage
Rax Sox2 DAPI
G
1st passage
Vimentin Nestin
H
1st passage
Bmi1 DAPI
I
1st passage
Lhx2 DAPI
J
1st passage
BLBP DAPI
K
1st passage
BrdU DAPI
L
1st passage
Rax Ki-67 DAPI
M
1st passage
FGFR1 DAPI
N
1st passage
pErk1/2 DAPI
O
1st passage
GFAP DAPI
P
1st passage
GLAST DAPI

Figure 6

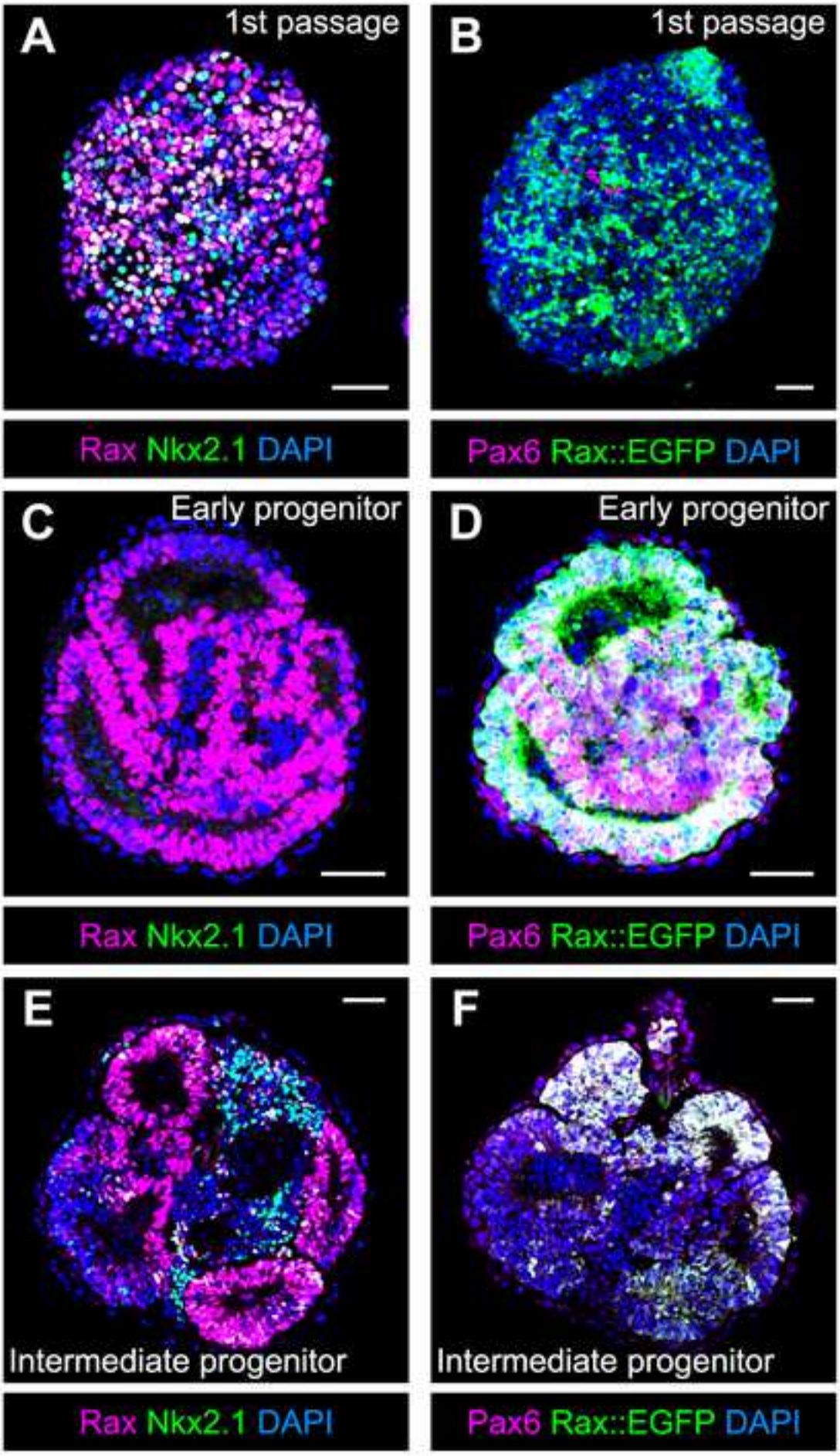
A
1st passage
Rax Nkx2.1 DAPI
B
1st passage
Pax6 Rax::EGFP DAPI
C
Early progenitor
Rax Nkx2.1 DAPI
D
Early progenitor
Pax6 Rax::EGFP DAPI
E
Intermediate progenitor
Rax Nkx2.1 DAPI
F
Intermediate progenitor
Pax6 Rax::EGFP DAPI

Figure 7

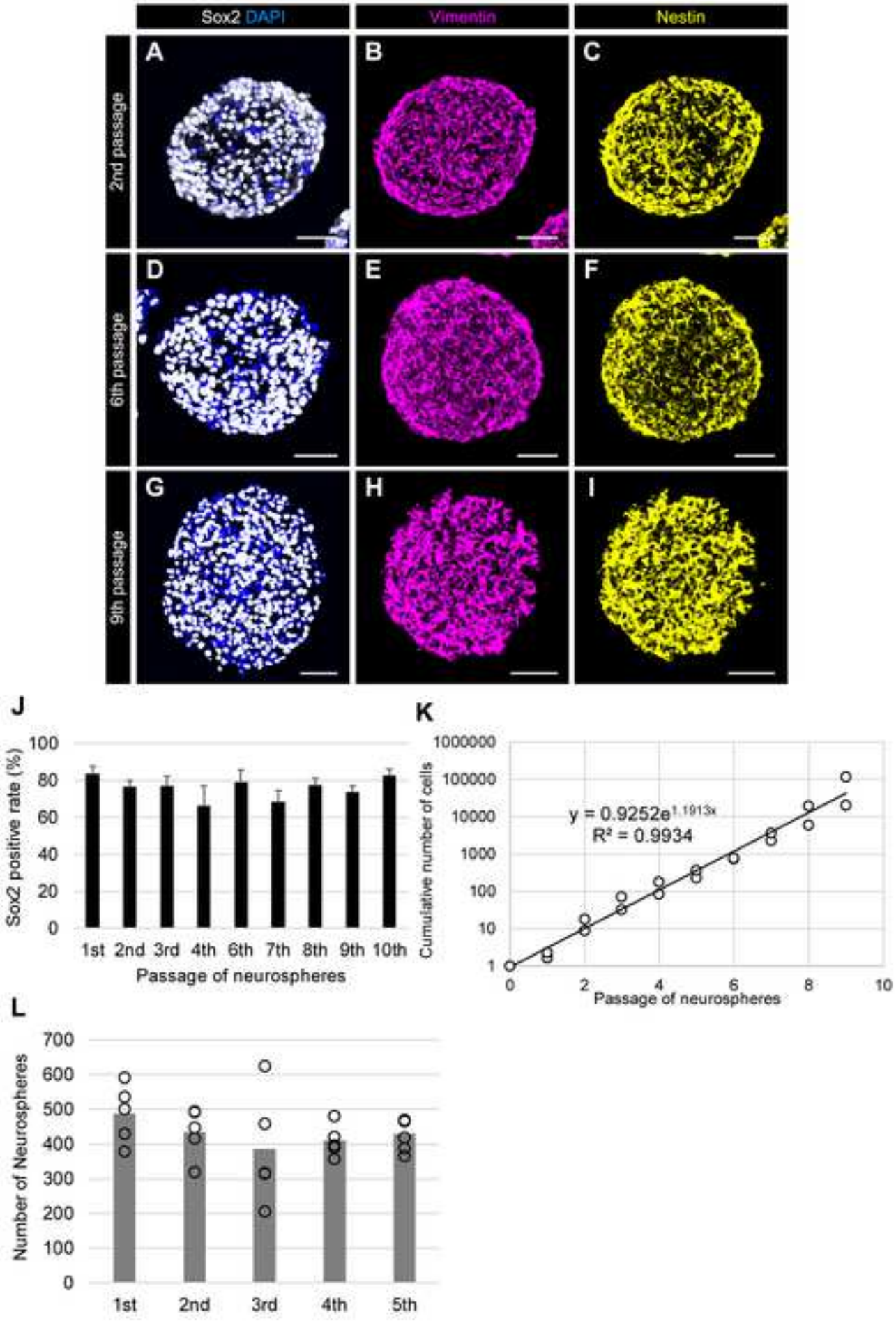
Sox2 DAPI
Vimentin
Nestin
2nd passage
6th passage
9th passage
A
B
C
D
E
F
G
H
I
J
Sox2 positive rate (%)
100
80
60
40
20
0
1st 2nd 3rd 4th 6th 7th 8th 9th 10th
Passage of neurospheres
K
Cumulative number of cells
1000000
100000
10000
1000
100
10
1
y = 0.9252e1.1913x
R² = 0.9934
0 2 4 6 8 10
Passage of neurospheres
L
Number of Neurospheres
700
600
500
400
300
200
100
0
1st 2nd 3rd 4th 5th

Figure 8

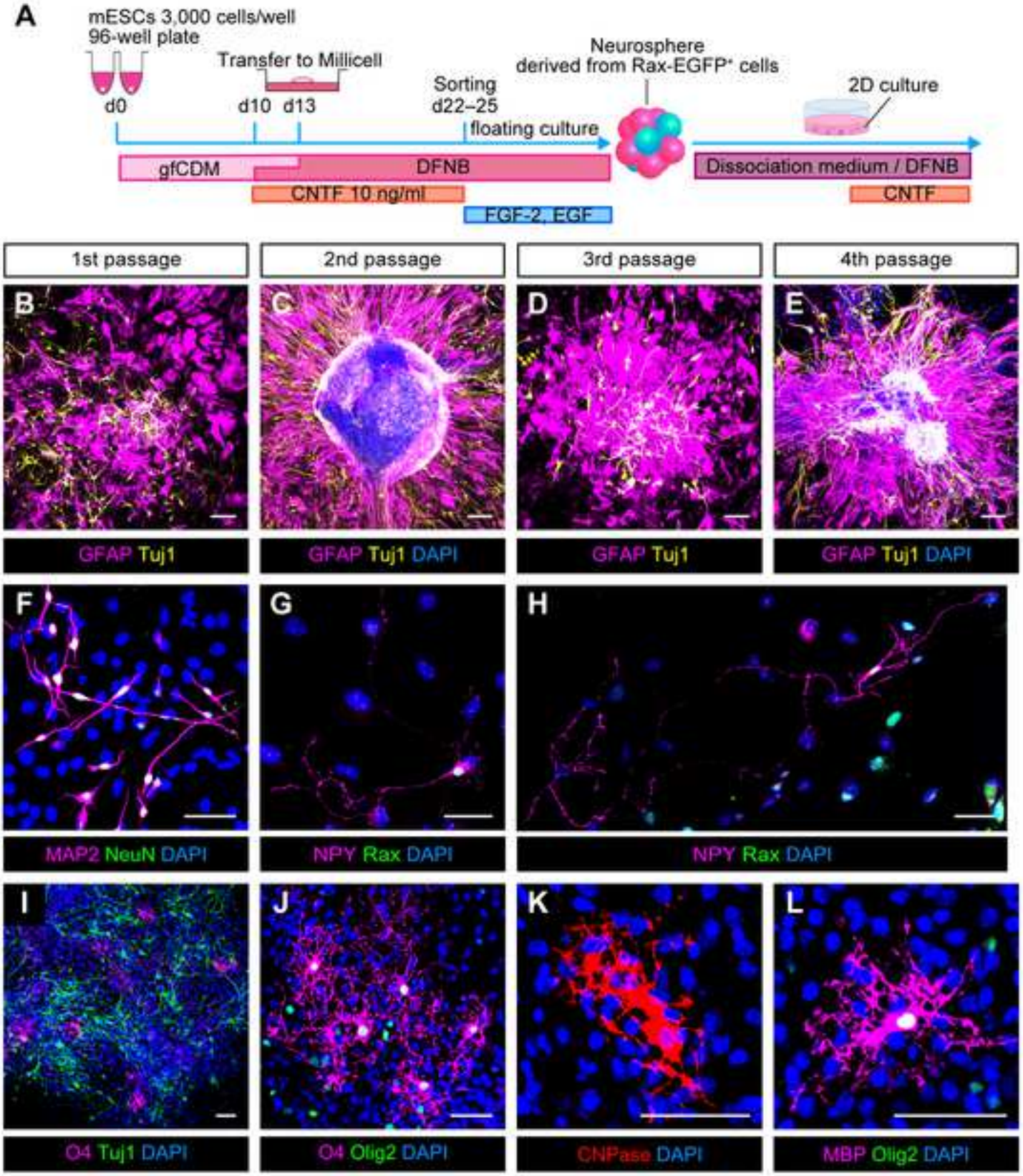
A
mESCs 3,000 cells/well
96-well plate
Transfer to Millicell
d0
d10 d13
Sorting
d22–25
Neurosphere
derived from Rax-EGFP+ cells
floating culture
2D culture
gfCDM
DFNB
CNTF 10 ng/ml
FGF-2, EGF
Dissociation medium / DFNB
CNTF
1st passage
2nd passage
3rd passage
4th passage
B
C
D
E
GFAP Tuj1
GFAP Tuj1 DAPI
GFAP Tuj1
GFAP Tuj1 DAPI
F
G
H
MAP2 NeuN DAPI
NPY Rax DAPI
NPY Rax DAPI
I
J
K
L
O4 Tuj1 DAPI
O4 Olig2 DAPI
CNPase DAPI
MBP Olig2 DAPI

Figure 9

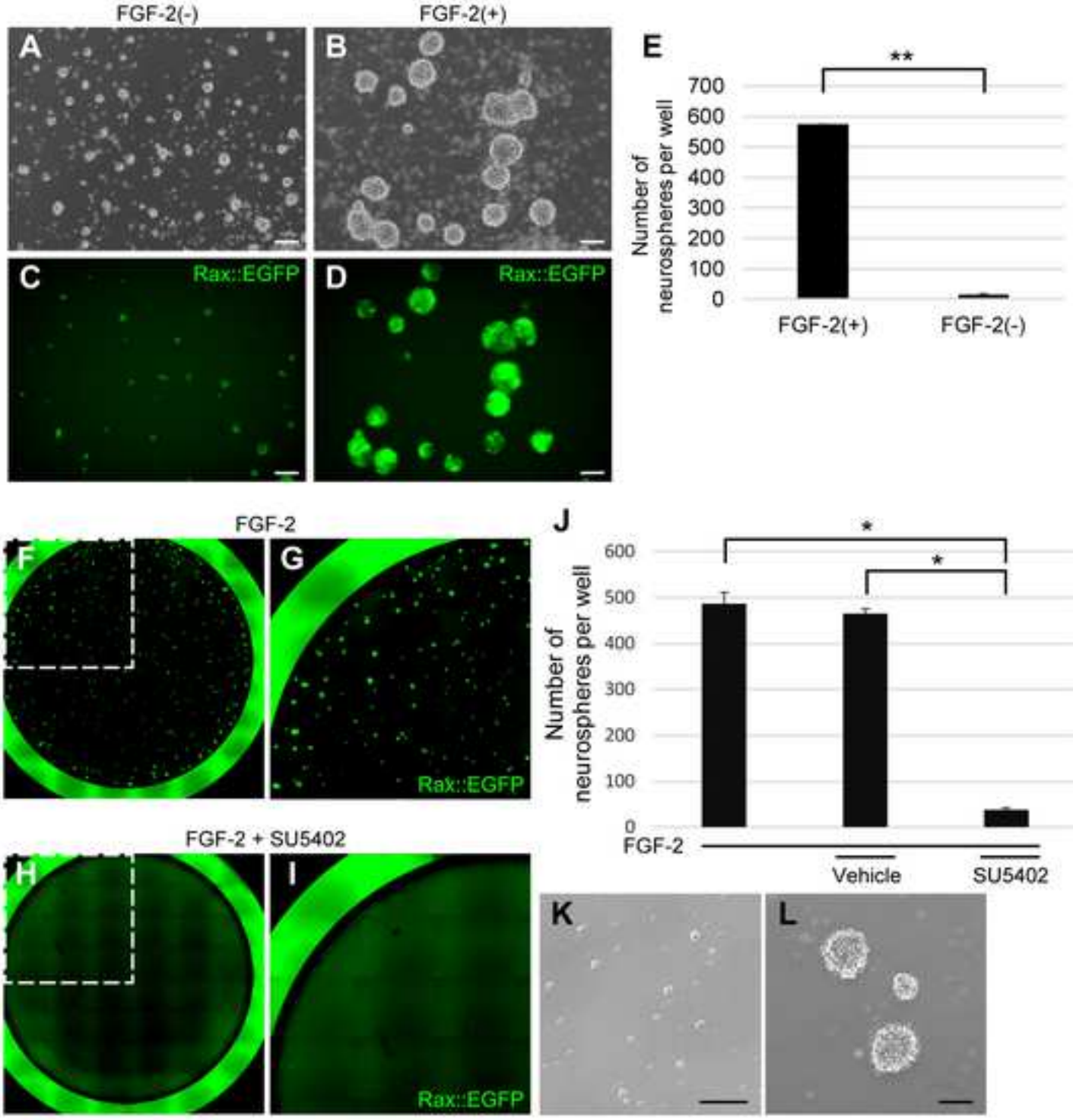
FGF-2(-)
FGF-2(+)
A
B
C
Rax::EGFP
D
Rax::EGFP
E
**
Number of neurospheres per well
700
600
500
400
300
200
100
0
FGF-2(+)
FGF-2(-)
FGF-2
F
G
Rax::EGFP
J
*
*
Number of neurospheres per well
600
500
400
300
200
100
0
FGF-2
Vehicle
SU5402
FGF-2 + SU5402
H
I
Rax::EGFP
K
L

Figure 10

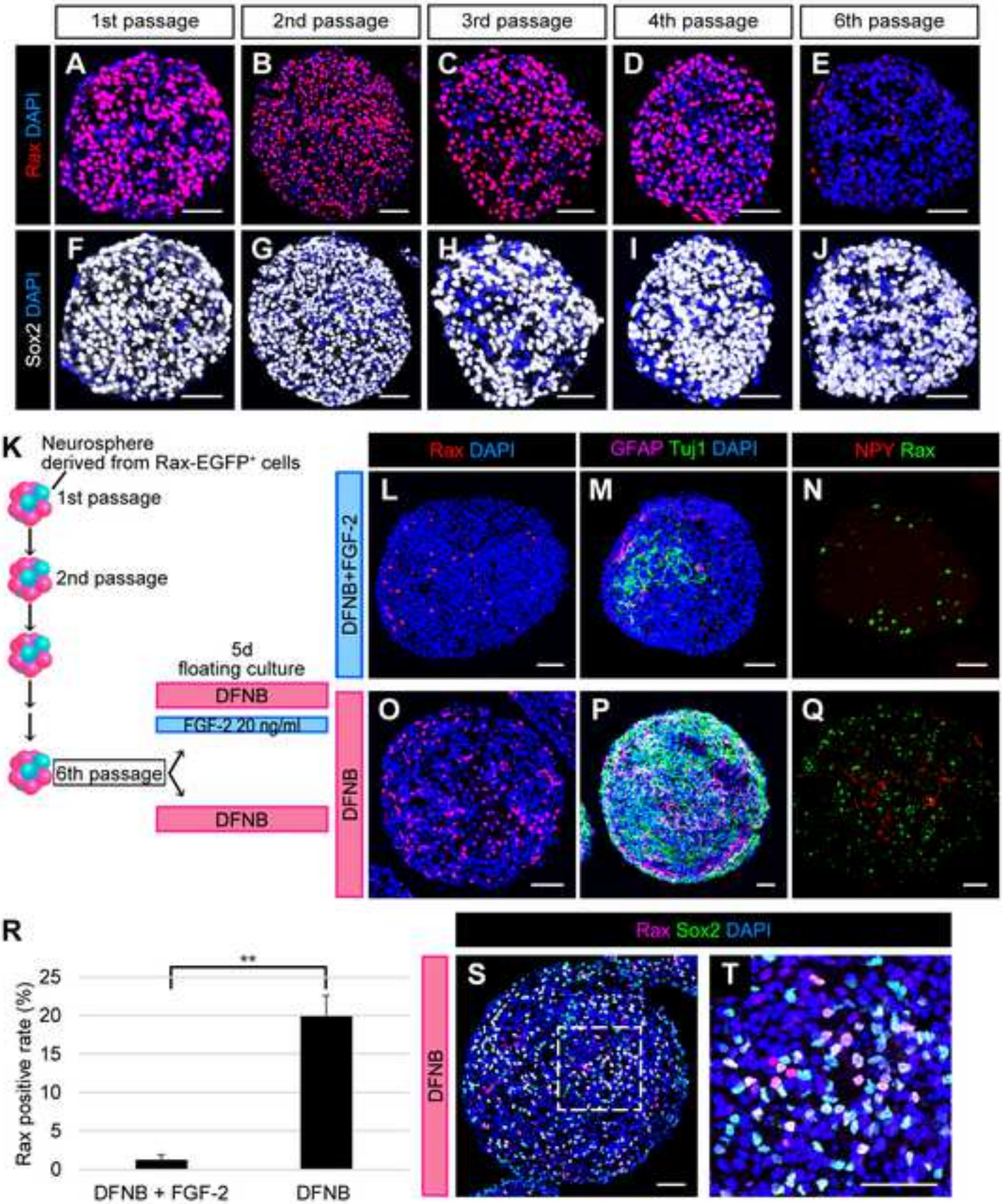
1st passage
2nd passage
3rd passage
4th passage
6th passage
Rax DAPI
Sox2 DAPI
A
B
C
D
E
F
G
H
I
J
K
Neurosphere
derived from Rax-EGFP+ cells
1st passage
2nd passage
5d
floating culture
DFNB
FGF-2 20 ng/ml
6th passage
DFNB
Rax DAPI
GFAP Tuj1 DAPI
NPY Rax
DFNB+FGF-2
L
M
N
DFNB
O
P
Q
R
Rax positive rate (%)
25
20
15
10
5
0
**
DFNB + FGF-2
DFNB
Rax Sox2 DAPI
DFNB
S
T